Re-evaluation of lysyl hydroxylation in the collagen triple helix: lysyl hydroxylase 1 and prolyl 3-hydroxylase 3 have site-differential and collagen type-dependent roles in lysine hydroxylation.

Short title: Two distinct mechanisms of LH1and P3H3 during collagen biosynthesis in the rER

Yoshihiro Ishikawa[1,2,#,*], Yuki Taga[3], Keith Zientek[2, $], Nobuyo Mizuno[2, ¶], Antti M. Salo[4], Olesya Semenova[2], Sara Tufa[2], Douglas R. Keene[2], Paul Holden[2], Kazunori Mizuno[3], Johanna Myllyharju[4] and Hans Peter Bächinger[1]

1: Department of Biochemistry and Molecular Biology, Oregon Health & Science University, Portland, Oregon, USA, 2: Shriners Hospital for Children, Research Department, Portland, Oregon, USA, 3: Nippi Research Institute of Biomatrix, Ibaraki, Japan, 4: Oulu Center for Cell-Matrix Research, Biocenter Oulu and Faculty of Biochemistry and Molecular Medicine, University of Oulu, Oulu, Finland.

Present address; #: Departments of Ophthalmology, University of California San Francisco, School of Medicine, California, USA, $: Proteomics core facility, Oregon Health & Science University, Portland, Oregon, USA, ¶: Vaccine and Gene Therapy Institute, Oregon Health and Science University, Portland, Oregon, USA.

*: Corresponding author: Yoshihiro Ishikawa, Ph.D., Department of Ophthalmology, University of California, San Francisco, School of Medicine, California, USA;
Tel: (503) 866-5940, E-mail: yoshi.molecularensemble@gmail.com
ORCID-ID: https://orcid.org/0000-0003-2013-0518

Competing Interests: The authors declare that they have no competing interests related to this work

Abstract

Collagen is the most abundant protein in humans and is heavily post-translationally modified. Its biosynthesis is very complex and requires three different types of hydroxylation (two for proline and one for lysine) that are generated in the rough endoplasmic reticulum (rER). These processes involve many enzymes and chaperones which were collectively termed the molecular ensemble for collagen biosynthesis. However, the function of some of the proteins in this molecular ensemble is controversial. While prolyl 3-hydroxylase 1 and 2 (P3H1, P3H2) are bona fide collagen prolyl 3-hydroxylases, the function of prolyl 3-hydroxylase 3 (P3H3) is less clear. A recent study of P3H3 null mice demonstrated that this enzyme had no activity as prolyl 3-hydroxylase but may instead act as a chaperone for lysyl hydroxylase 1 (LH1). LH1 is required to generate hydroxylysine for crosslinking within collagen triple helical sequences. If P3H3 is a LH1 chaperone that is critical for LH1 activity, P3H3 and LH1 null mice should have similar deficiency in lysyl hydroxylation. To test this hypothesis, we compared lysyl hydroxylation in type I and V collagen from P3H3 and LH1 null mice. Our results indicate LH1 plays a global role for lysyl hydroxylation in triple helical domain of type I collagen while P3H3 is indeed involved in lysyl hydroxylation particularly at crosslink formation sites but is not required for all lysyl hydroxylation sites in type I collagen triple helix. Furthermore, although type V collagen from LH1 null mice surprisingly contained as much hydroxylysine as type V collagen from wild type, the amount of hydroxylysine in type V collagen was clearly suppressed in P3H3 null mice. In summary, our study suggests that P3H3 and LH1 likely have two distinct mechanisms to distinguish crosslink formation sites from other sites in type I collagen and to recognize different collagen types in the rER.

Author summary

Collagen is one of the most heavily post-translationally modified proteins in the human body and its post-translational modifications provide biological functions to collagen molecules. In collagen post-translational modifications, crosslink formation on a collagen triple helix adds important biomechanical properties to the collagen fibrils and is mediated by hydroxylation of very specific lysine residues. LH1 and P3H3 show the similar role in lysine hydroxylation for specific residues at crosslink formation sites of type I collagen. Conversely, they have very distinct rules in lysine hydroxylation at other residues in type I collagen triple helix. Furthermore, they demonstrate preferential recognition and modification of different collagen types. Our findings provide a better understanding of the individual functions of LH1 and P3H3 in the rER and also offer new directions for the mechanism of lysyl hydroxylation followed by crosslink formation in different tissues and collagens.

Introduction

Collagen is not only the most abundant protein, but is also one of the most heavily post-translationally modified proteins in the human body [1, 2]. These post-translational modifications (PTMs) play essential roles in providing biological functions to collagen molecules. Two distinct classifications of PTM exist prior to the incorporation of collagen into extracellular matrices (ECMs), occurring in the unfolded state (a single α-chain) in the rough endoplasmic reticulum (rER) and the folded state (triple helical structure) in the Golgi and the ECM space [3, 4]. Interestingly, there is the case that the extent of the PTM in the Golgi and the ECM space is governed by the PTMs in the rER. Crosslink formation is an important PTM occurring on a collagen triple helical structure and adds important biomechanical properties to the collagen fibrils [5, 6]. However, the pathway of crosslink formation in type I collagen depends on the presence and absence of lysyl hydroxylation in both the collagenous and the telopeptide region [7, 8]. Additionally, *O*-glycosylation, which is generated after lysyl hydroxylation, is involved in crosslink formations and the amount depends on the type of tissue, the rate of triple helix formation and the presence or absence of ER chaperones [9-12]. Thus, PTMs of unfolded α-chains in the rER are critical for quality control in a collagen ultrastructure.

Collagen biosynthesis including PTMs is complex and involves many enzymes and chaperones, which are collectively termed the molecular ensemble [13]. Because some of the enzymes only can modify unfolded, and not triple helical, collagen chains the time that collagen chains remain unfolded in the rER is a critical factor for correct PTMs and foldases control the rate of triple helix formation [14-17]. There are three hydroxylations (proline 3-hydroxylation, proline 4-hydroxylation and lysine hydroxylation) that are fundamental PTMs occurring before triple helix formation [3, 13]. Interestingly, the function of prolyl 3-hydroxylase 3 (P3H3) is controversial. It has been suggested that this protein has no prolyl hydroxylase activity and instead acts as a chaperone for lysyl hydroxylase 1 (LH1) [18]. LHs hydroxylate specific lysine residues in both the collagenous and telopeptide regions, and the three isoforms (LH1, 2 and 3) have been proposed to play specific roles based on collagen sequences [16]. LH2 is specific for hydroxylating the telopeptide [16], and LH1 has been suggested to hydroxylate the triple-helical regions [13, 19-21]. The study of patients with LH1 mutations, and of LH3 mutant mice indicate that both LH1 and LH3 could have substrate preferences (e.g. LH1 and LH3 prefer type I/III collagen and type II/IV/V collagen, respectively) [22-25]. However, this indication could not fully explain the diversity of lysyl hydroxylation in tissues of the LH1 null mouse model and type I collagen from different tissues of Ehlers-Danlos Syndrome (EDS)-VIA patients [23, 26]. Few analyses have investigated the level of lysyl hydroxylation in purified collagens from mutant or LH knockout models using both qualitative and quantitative measurements.

In this study, we aimed to re-evaluate the role of LH1 in collagen triple helices and test whether P3H3 is essential for the LH1 activity. To achieve this, we compared the levels of overall lysyl hydroxylation and PTM occupancy at individual sites between collagens extracted from P3H3 or LH1 null mice. If P3H3 is a chaperone required for LH1 activity as recently suggested [18], then both P3H3 and LH1 null mice should cause similar defects in lysine hydroxylation. Moreover we analyzed different collagens from different tissues to test the hypothesis that LH1 is a collagen type-specific enzyme [22-25], and to understand if P3H3 might contribute to this differential activity. This direct comparison of different collagens from different tissues from these two null mouse lines provide a better understanding of the individual functions of P3H3 and LH1 in the rER.

Results

Basic characterization of P3H3 null mice – P3H3 null mice were generated by Ozgene as shown in Figure 1A and with more detailed information in the methods section. Figure 1B displays the result of PCR genotyping showing that the P3H3 null allele product is smaller than WT due to the deletion of Exon 1. To confirm that the expression of P3H3 protein was abolished, Western blotting was performed using a whole kidney lysate and the protein signal corresponding to MW of P3H3 (79 kDa) was absent in the P3H3 null lysate (Figure 1C). As previously reported [18], P3H3 null mice were also viable and we did not observe any obvious growth or skeletal phenotypes by growth curves and X-ray images, respectively (Figure 1D and E). LH1 null mice were generated and characterized previously [26].

Biochemical characterization of purified type I collagen from different tissues of P3H3 and LH1 null mouse models – To enable qualitative and quantitative analyses, type I collagen was purified from tissues by pepsin treatment followed by sodium chloride precipitation. We analyzed three different tissues (tendon, skin and bone) from each mouse model. We evaluated the level of PTMs by comparing migration using SDA-PAGE [27] and determined the thermal stability using circular dichroism (CD) spectra [28, 29] of purified type I collagen from the different tissues of P3H3 null and LH1 null mice (Figure 2). Type I collagen from both P3H3 null and LH1 null skin migrates a little faster and shows a lower melting temperature than WT, whereas there is no clear difference for type I collagen from tendon and bone between WT and nulls in gel migration or melting temperature (Figure 2). This suggests that skin is the most affected tissue in both P3H3 null and LH1 null mice.

Quantitative analysis to determine the total level of post-translational modifications of type I collagen in P3H3 null and LH1 null mice – Amino acid analysis (AAA) was used to quantify the total number of PTMs in the purified type I collagens. Neither P3H3 nor LH1 null mice had changes in proline hydroxylations (prolyl 3- and 4-hydroxylation), however, both strains had interesting changes in lysyl hydroxylation (Figure 3 and Table 1). LH1 deficiency significantly decreased the amounts of hydroxylysine in tendon, skin and bone although bone was a slightly lesser extent. In contrast, P3H3 deficiency had a much smaller effect on lysyl hydroxylation than LH1 whereby skin showed further reduction of hydroxylysine compared to tendon and bone. Next, we determined the occupancy of *O*-glycosylation of hydroxylysine in tendon and skin by liquid chromatography–mass spectrometry (LC–MS). The calculated value of galactosyl hydroxylysine (GHL) does not show any significant difference in skin but does slightly increase in tendon for both P3H3 null and LH1 null mice (Figure 4 and Table 2). Interestingly, the magnitude of change in unmodified hydroxylysine and glucosylgalactosyl hydroxylysine (GGHL) seems to have some correlation in both tendon and skin. For example, both P3H3

null and LH1 null type I collagen in tendon showed unmodified hydroxylysine was decreased whereas GGHL was increased by a similar magnitude of decreasing unmodified hydroxylysine (Figure 4 and Table 2). While the effect is opposite manner, the same observation is also seen in skin of P3H3 null and LH1 null type I collagen (Figure 4 and Table 2). This indicates that the affected site(s) in the absence of P3H3 and LH1 are different location or have different level of *O*-glycosylation between tendon and skin. Taken together, P3H3 clearly has a role in lysyl hydroxylation, but the level of lysyl hydroxylation in type I collagen is more drastically decreased in LH1 null mice compared to P3H3 null mice. Furthermore, the data also suggests that P3H3 and LH1 likely have distinct roles in lysyl hydroxylation and sugar attachment between tissues.

Individual lysyl hydroxylation site analysis of type I collagen from P3H3 null and LH1 null tissues – The α1 and α2 chain of type I collagen contain multiple lysyl hydroxylation sites in their triple helical sequences [30-32]. A previous report of P3H3 null mice [18] only demonstrated lysyl hydroxylation sites on lysine-87 (K87) in both the α1 and α2 chain. These residues at the amino-terminus of triple helical domain are important for crosslink formation in the ECM [18]. We determined the occupancy of PTMs at individual lysyl hydroxylation sites between WTs, P3H3 and LH1 nulls in tendon and skin (Figure 5, Table 3 and Table 4). In LH1 null tissues, the level of lysyl hydroxylation and subsequent *O*-glycosylation were significantly decreased at all lysyl hydroxylation sites of both tendon and skin. In P3H3 null tissues, we confirmed the reduction of lysine modifications in K87 in both the α1 and α2 of type I collagen as previously reported [18], and a large reduction was also found at α1 K930 and α2 K933 which are near the carboxy-terminus of the triple helical domain involved in crosslink formation. The other sites α1 K99, α1 K174, α2 K174 and α2 K219 also showed clear reduction, however, there was no notable decrease in the level of lysyl hydroxylation at the sites in the middle of the triple helix of α1 chain (α1 K219 and α1 K564). In summary, LH1 might play a global role for lysyl hydroxylation at all sites in the triple helical domain of type I collagen whereas the role of P3H3 could be restricted to specific sites.

Qualitative and quantitative characterization of skin type V collagen from WT, P3H3 null and LH1 null mice– Type V collagen is heavily lysyl hydroxylated and *O*-glycosylated and abundant in skin compared to tendon and bone [33]. We isolated type V collagen from skin of P3H3 and LH1 null mice and subjected it to gel migration analysis. Although type V collagen from LH1 null mice did not show a clear difference in gel migration however, type V collagen from P3H3 null mice appeared to migrate faster compared to WT (Figure 6A). To confirm these observations, we identified the level of PTMs in both P3H3 null and LH1 null type V collagens by AAA. The ratio in prolyl hydroxylations is slightly different between control animals from the P3H3 and LH1 mouse strains (Figure 6B). One potential

explanation is that the analyses were done on skin from 2~5-month-old and 10-week-old mice for P3H3 and LH1 mice, respectively (more detailed information in the methods section). Similar to type I collagen, neither P3H3 nor LH1 null mice had changes in proline hydroxylations (prolyl 3- and 4-hydroxylation). Surprisingly, P3H3 null mice, but not LH1 null mice, had reduced levels of lysyl hydroxylation in type V collagen isolated from skin (Figure 6B and Table 1) however the occupancy of *O*-glycosylation on hydroxylysine was not changed (Table 2). The reduced lysyl hydroxylation in P3H3 null mice influenced the thermal stability of type V collagen and CD melting curves showed only one of the two thermal transitions seen in WT (Figure 6C). Since lysine residues at the Yaa position of collagenous Gly-Xaa-Yaa triplets are extensively glycosylated in type V collagen [33], site-specific characterization of lysine modifications was difficult due to missed cleavage at hydroxylysine glycosides by trypsin [34]. We were able to analyze two sites, α1(V) K84 and α2(V) K87 (Figure 7 and Table 5), that are involved in crosslink formation [35]. At both sites, the level of GGHL was decreased and the magnitude of reduction of GGHL corresponds to that of the increased unmodified lysines in the absence of P3H3, however this change at α1(V) K84 was not significant statistically (Table 5). This suggests P3H3 could play an important role in lysyl hydroxylation and/or subsequent *O*-glycosylation at the site of crosslink formation consistently. In LH1 null mice, there was a marginal change at α1(V) K84, however, α2(V) K87 was clearly affected. Potential explanation is that the α2-chain of type V collagen is classified as an A-clade chain, which includes both the α1- and α2-chain of type I collagen, whereas the α1-chain of type V collagen belongs to B-clade [36, 37]. LH1 seems to hydroxylate the α2(V) K87 preferentially. Nevertheless, the ratio of two α1-chains and one α2- chain in type V collagen could hide the effect caused by impaired LH1 activity and not show any distinct difference in type V collagen between WT and LH1 null observed in Figure 6B. In summary, P3H3 is required for proper lysyl hydroxylation of type I and type V collagen whereas LH1 is dispensable for lysyl hydroxylation in skin type V collagen.

Skin analysis in P3H3 null mice – Consistent with skin type V collagen analysis, and as reported previously [18], we found defects in skin from P3H3 null mice. Masson's Trichrome staining shows less collagen content and the thickness and ratio were altered in the dermis and hypodermis (Figure 8A – C). Electron microscopy showed that the average diameter of collagen fibrils is similar between P3H3 null (84.9 ± 35.6 nm) and WT (85.1 ± 25.9 nm) (Figure 8D), however the distribution of fibril diameters was broader in P3H3 null (Figure 8E) and this was also reported in LH1 null skin [26]. In summary, a precise number of PTMs in the rER is required to maintain an appropriate ultrastructure in collagen rich tissues.

Discussions

In the rER, many enzymes and post-translational modifiers interact with molecular chaperones via either strong or weak affinity interaction to improve their functions [38, 39]. In particular, the molecular ensemble for collagen biosynthesis consists of variety of protein–protein interactions [13, 40]. When an interaction is impaired, as found in genetic disorders, the magnitude of the impact depends on what type of protein–protein interaction is disrupted. Prolyl 3-hydroxylase 1 (P3H1), cartilage-associated protein (CRTAP) and cyclophilin B (CypB) form a complex with very tight molecular interactions [41, 42]. In this complex each protein stabilizes the others and CRTAP requires the other two proteins to maintain its solubility [42-44]. As a result, the lack of one molecule in this complex leads to very similar phenotypic abnormalities in osteogenesis imperfecta (OI) [20, 45]. On the other hand, CypB is also identified as a binding partner for LH1. CypB is an ER-resident peptidyl-prolyl cis-trans isomerase and was the first molecule shown to be associated with LH1 [46]. The absence of CypB or disruption of the interaction with LH1 results in the reduction of lysyl hydroxylation in tendon and skin [31, 32], while the amount of lysyl hydroxylation is increased in bone [47]. Additionally, there is a site-specific effect to the level of lysyl hydroxylation in tendon, skin and bone. Therefore CypB was proposed to control lysyl hydroxylation [32]. SC65, a homolog of CRTAP, was suggested to be interacting with P3H3 with relatively strong affinity as indicated by gel filtration chromatography combined with Western blots [48]. In the SC65 null mouse, a reduction of lysyl hydroxylation at α1(I) and α2(I) K87 was found in tissues, whereas these changes did not always correspond to the changes found in P3H3 null mice [18]. Overall, mouse models of LH1 and LH1-associated proteins showed aberrant crosslink formations caused by lysine under hydroxylation at the α1 K87 and α1 K930, therefore three molecules (CypB, SC65 and P3H3) have been proposed to form a complex with LH1 in the rER [48]. However, it is not clear how these molecules interact with each other and what effect one has on other molecules.

To evaluate the correlation between LH1 and one of the LH1-associated proteins, P3H3, we conducted quantitative analyses and directly compared the level of PTMs between WT, P3H3 null and LH1 null mouse tissues. Our results suggest that if P3H3 acts as a LH1 chaperone, this chaperone function is not required for all LH1 sites, as very specific sites related to crosslink formation in type I collagen were affected (Figure 5). Figure 9 represents the magnitudes of change of unmodified lysine residues in individual lysyl hydroxylation sites between three different null mouse models compared to WT. These observations imply that both P3H3 and CypB play important roles for the function of LH1 and that a lack of even one of the components attenuates the amounts of hydroxylysine in the crosslink formation sites. Conversely, other lysyl hydroxylation sites demonstrate very diverse effects between P3H3 null, LH1 null and CypB null mouse tissues. There are specific patterns that are changed in each null mouse model. Modified lysine residues were hardly found in LH1 null, whereas P3H3 null showed normal or slightly increased unmodified lysine residues. In contrast, CypB null showed normal or

decreased unmodified lysine residues despite increasing unmodified lysine residues at crosslink formation sites as well as P3H3 and LH1 nulls. Moreover, additional sugar attachments are found at other lysyl hydroxylation sites (e.g. K174 and K219) in the P3H1 null mice model [30] which displays an OI phenotype [49] and CypB null is also a model of recessive type IX OI [47]. This suggests that these proteins do not form a tight molecular complex like the P3H1/CRTAP/CypB complex but more likely a combination of distinct protein–protein interactions. Indeed, this variety of interactions was shown by Western blotting results between LH1 and three LH1 associated protein. The protein level of P3H3 was not abolished but decreased in the absence of CypB and SC65 [32, 48]. Similarly, SC65 protein was affected in CypB null mice [32]. However, the protein level of LH1 was decreased as well as P3H3 in the absence of SC65 whereas the lack of CypB interestingly induced more LH1 protein than WT [32, 48]. Additionally, size exclusion chromatography demonstrated that P3H3 and SC65 were possibly associated in a tight interaction like the P3H1/CRTAP/CypB complex, however neither LH1 nor CypB was a part in this tight interaction [48]. We imagine a very precise molecular interplay is required particularly around crosslink formation sites and this is not simply determined as chaperone effects and/or a complex formation. Collectively, we would like to term this precise mechanism as a "local molecular ensemble". We looked for the specific binding or enhancer sequences of type I collagen near lysyl hydroxylation sites based on our results (Figure 10). As a previous report suggested [32], the KGH sequence occurs at or near crosslink formation sites to provide preferential interaction sites for the CypB-involved SC65/P3H3 ER complex to facilitate LH1 activity. This hypothesis is possible, but cannot explain the reduction of α2(I) K87, K174 and K933 since the KGH sequence only exist near α2(I) K87 in mouse and does not exist near α2(I) K174. (Figure 10). Interestingly, some ECM proteins (integrins, decorin and SPARC) are likely associated at around K174 of type I collagen [50]. Thus, α2(I) K174 could have important roles since this site is highly sensitive in the absence of P3H3, LH1 and CypB (Figure 9). In type V collagen, both α1(V) K84 and α2(V) K87 are involved in crosslink formation [35] and these site are also the KGH sequence (Figure 10). However, the effects at these sites are not consistent between P3H3 and LH1 null (Figure 7). Further studies are required to elucidate how these four molecules properly distinguish and gather to form a local molecular ensemble at individual lysyl hydroxylation sites at a molecular level. Here we note that a previous report showed the difference in PTMs at α1(V) K87 [18], however the actual residue 87 is arginine instead of lysine as we showed above and this is also confirmed by database (UniProt entry numbers: P20908 for human and O88207 for mouse, NCBI accession number: bovine for XP_024855494).

The previous studies of LH1 null and EDS type VIA patients suggested tissue specific and collagen type specific lysyl hydroxylation could exist since different magnitudes of reduction in lysyl hydroxylation between tissues was found [22-25]. Potential explanations were suggested such as the

complexity of different collagen types between tissues, a distribution in the expression and/or protein levels of LH isoenzymes or a compensation by two other LH isoenzymes, which could hydroxylate the peptides containing the sequences of hydroxylation sites in triple helices of type I and type IV collagen [9, 16, 51]. Here, we show that the purified type I collagen without telopeptide regions of tendon, skin and bone from LH1 null are differentially modified between tissues (Figure 3). We also find a decrease of total amount of hydroxylysine in type I collagen from P3H3 null mouse tissues, however the decrease was less than in LH1 null mouse tissues (Figure 3). In contrast to LH1 null and P3H3 null, CypB null mice showed the tissue dependent alteration in total amount of hydroxylysine. Hydroxylysine was reduced in type I collagen from tendon and skin while an increase was observed in bone [31, 32, 47]. Therefore, lysyl hydroxylation in triple helical domain of type I collagen is likely reactive by disruption of LH1 and LH1 associated proteins. Contrary to the results found in type I collagen, there was interestingly no significant difference in type V collagen from LH1 null skin [26]. Surprisingly, P3H3 null showed an obvious reduction of lysyl hydroxylation in type V collagen from skin as well as type I collagen (Figures 3 and 6). Considering the results from the lung and kidney of LH3 mutant mice that demonstrate that the amount of hydroxylysine was not changed in type I collagen rich fractions, but was reduced by 30% in type IV and type V collagen rich fractions [24], we suggest that LH1 and LH3 have a substrate specificity for at least type I collagen and type V collagen, respectively. In addition, given that the LH3 mutant mice only showed a decrease of 30% in type IV and type V collagen rich fractions, that type V collagen from P3H3 null showed a decrease of hydroxylysine content and also that the hydroxylysine content of bone type I collagen was decreased in P3H3 null despite increasing in CypB null, we speculate that P3H3 might have a lysyl hydroxylation activity, namely, LH4 like enzyme in the rER. Although P3H3 belongs to the prolyl 3-hydroxylase family, no substrate or enzyme activity have been identified. P3H3 could interact with both LH1 and LH3, however this is unlikely because the phenotype of P3H3 null mice is very mild. Thus, direct prolyl and lysyl hydroxylase activity assays are needed to determine if P3H3 acts as prolyl and/or lysyl hydroxylase. However, attempts to produce necessary quantities of recombinant protein have not succeeded.

In conclusion, P3H3 and LH1 play critical roles to hydroxylate lysine residues in crosslink formation sites in type I collagen whereas they likely have distinct mechanisms to modify other sites in type I collagen and to recognize different collagen types in the rER. Indeed, it is still unclear what the most important factors are to obtain the precise PTMs in collagens: is it the formation of specific protein–protein interactions or the level of expression that leads to the existence of active complexes? Our findings offer new directions for the understanding of lysyl hydroxylation in different tissues and in different collagens and provide a new interpretation of previous findings in LH1 null mice, LH3 null mice and EDS VI patients.

Experimental procedures

P3H3 null mice – P3H3 null mice were purchased from Ozgene (Bentley, Australia). Directed knockouts were created in which exon 1 of the mouse *Leprel2* (also called *P3H3*) gene (UniProt entry number: Q8CG70), coding P3H3, were deleted. The procedure is briefly described as follow. The PGK-neo selection cassette flanked by FRT sites was generated by PCR from C57BL/6 genomic DNA and inserted into the downstream of the exon 1 which was flanked by loxP sites. The targeted locus was eliminated using an FLP recombinase and a Cre recombinase. ES cell clones were confirmed by southern hybridization. P3H3 inactivation was verified in mice by DNA preparation from tissues and PCR with primer sets (Fwd: 5'-CTTACCCACACTAGACCCATGTGTC-3' and Rev: 5'-GTTGCATTCATTAGCCTAGACCCGCTA-3'). PCR was performed at least 30 times and the PCR products for wild type and null were located at around 1,000 and 200 pb, respectively. Tissues were harvested from 2~5-month-old mice for collagen analysis, 8-month-old mice for skin staining analysis and 3-month-old mice for fibril diameter analysis.

LH1 null mice – Plod1 knockout mice were produced as described earlier [26] using in-frame insertion of lacZ-neo cassette into exon 2. Mice were further backcrossed into C57BL/6N background. Genotyping was done by PCR [26] and tissues were harvested from 10-week-old mice for collagen analysis.

Western Blotting – A kidney was extracted from wild type, heterozygous and null P3H3 mouse and homogenized using T-PER (Thermo Fisher Scientific) containing protease inhibitors at 4 °C. After centrifugation, soluble proteins in the extract were mixed with NuPAGE LDS sample buffer with reducing agents. These protein solutions were separated by Bolt 4-12% Bis-Tris Plus (Life Technology) and electrotransferred onto PVDF membranes. Antibodies were incubated to detect the specific protein after the membranes were blocked in PBS solution containing 5% (w/v) skim milk. All proteins were detected by alkaline phosphatase developed with 5-bromo-4-chloro-3-indolyl phosphate and Nitro blue tetrazolium. Rabbit polyclonal antibody against P3H3 (*LEPREL2*) and rabbit polyclonal antibody against GAPDH were purchased from Proteintech (16023-1-AP) and Sigma-Aldrich (PLA0125), respectively. Alkaline phosphatase-conjugated anti-rabbit IgG (A9919: Sigma-Aldrich) was used as secondary antibody. Western blotting was performed three times using independently prepared three independent kidneys.

X-ray scan – X-rays were performed at least three times on independently prepared adult mice using a Faxitron cabinet instrument (model #43855B) made by Hewlett Packard. Voltages and exposure times were optimized for best resolution images.

Collagen Extraction from Tissues – Tendon, skin and bone were taken from adult mice. All procedures were performed at 4 ºC. Tendon and skin were incubated in excess volume of 0.1 M acetic acid with shaking for several hours. Ground bone in liquid nitrogen was incubated in 1.0 M acetic acid containing 0.05 M EDTA. Pepsin was added to a final concentration of 0.25 mg/mL and tissues were digested overnight. For bone, pepsin digestion and decalcification were taken three days. The solutions were centrifuged to remove insoluble material, and then NaCl was added to a final concentration of 0.7 M to precipitate collagens and the solution was incubated overnight. Precipitates were collected by centrifugation at 13,000 rpm for 15 min and resuspended in 0.1 M acetic acid. This solution was enriched type I collagen from tendon and bone and was dialyzed against 0.1 M acetic acid to remove remaining NaCl. For skin, the solution was dialyzed in excess volume of 0.1 M Tris/HCl containing 1.0 M NaCl, pH 7.8 and then NaCl was added to a final concentration of 1.8 M to remove type III collagen. This solution was centrifuged at 13,000 rpm for 30 min and additional NaCl was added to a final concentration of 2.4 M to the supernatant. After incubating overnight, the solution was centrifuged at 13,000 rpm for 30 min. The pellets containing skin type I collagen was resuspended in 0.1 M acetic acid and dialyzed against 0.1 M acetic acid to remove remaining NaCl. Skin type V collagen was extracted using the supernatant of 0.7 M NaCl precipitation and additional NaCl was added to a final concentration of 4.0 M. After incubating overnight, the solution was ultra-centrifuged at 30,000 rpm for 30 min. The pellets containing skin type I collagen was resuspended in 0.1 M acetic acid and dialyzed against 0.1 M acetic acid to remove remaining NaCl.

Circular Dichroism – Circular dichroism spectra were recorded on an AVIV 202 spectropolarimeter (AVIV Biomedical, Inc., Lakewood, NJ) using a Peltier thermostatted cell holder and a 1-mm path length rectangular quartz cell (Starna Cells Inc., Atascadero, CA). The temperature scanning curves were monitored at 221 nm with 10 ºC/h scan rate. All curves were the average of at least three and two independent measurements using independently prepared collagen from tissue for type I and type V collagen, respectively.

Amino Acid Analysis – Acid hydrolysis was performed in 6 x 50-mm Pyrex culture tubes placed in Pico Tag reaction vessels fitted with a sealable cap (Eldex Laboratories, Inc., Napa, CA). Samples were placed in culture tubes, dried in a SpeedVac (GMI, Inc. Albertville, MN), and then placed into a reaction vessel that contained 250 ml of 6 M HCl (Pierce) containing 2% phenol (Sigma-Aldrich). The vessel was then purged with argon gas and evacuated using the automated evacuation workstation Eldex hydrolysis/derivatization workstation (Eldex Laboratories, Inc.). Closing the valve on the Pico Tag cap

maintained the vacuum during hydrolysis at 105 °C for 24 h. The hydrolyzed samples were then dried in a Savant SpeedVac. The dried samples were dissolved in 100 ml of 0.02 M HCl containing an internal standard (100 µM norvaline; Sigma). Analysis was performed by ion exchange chromatography with postcolumn ninhydrin derivatization and visible detection (440 nm/570 nm) with a Hitachi L-8800A amino acid analyzer (Hitachi High Technologies America, Inc., San Jose, CA) running the EZChrom Elite software (Scientific Software, Inc., Pleasanton, CA). Three technical replicates were performed in each analysis.

Glycosylation analysis – Glycosylation of hydroxylysine was estimated by LC–MS after alkaline hydrolysis as described previously [52]. In brief, type I and type V collagen samples were subjected to alkaline hydrolysis (2 N NaOH, 110 °C for 20 h under N_2) after adding stable isotope-labeled collagen as an internal standard. The alkaline hydrolysates were neutralized with 30% acetic acid and then desalted using a mixed-mode cation-exchange sorbent (Oasis MCX; Waters, Milford, MA). Unmodified and glycosylated hydroxylysines were quantitated by LC–MS in multiple reaction monitoring mode using a 3200 QTRAP hybrid triple quadrupole/linear ion trap mass spectrometer (AB Sciex, Foster City, CA) coupled to an Agilent 1200 Series HPLC system (Agilent Technologies, Palo Alto, CA) with a ZIC-HILIC column (3.5 µm particle size, L × I.D. 150 mm × 2.1 mm; Merck Millipore, Billerica, MA).

Site-Specific Characterization of Lysine PTMs – Site occupancy of lysine PTMs was estimated by LC–MS after protease digestion as described previously [32]. In brief, type I collagen samples were digested with trypsin (Promega, Madison, WI) or with collagenase from *Grimontia hollisae* (Wako Chemicals, Osaka, Japan) and pepsin (Sigma-Aldrich) after heat denaturation at 60 °C for 30 min. On the other hand, type V collagen samples were separated by SDS-PAGE, and the region containing α1(V) and α2(V) were subjected to in-gel digestion with trypsin. The protease digests of type I and type V collagen were analyzed by LC–MS on a maXis II quadrupole time-of-flight mass spectrometer (Bruker Daltonics, Bremen, Germany) coupled to a Shimadzu Prominence UFLC-XR system (Shimadzu, Kyoto, Japan). Site occupancy of each modification site was calculated using the peak area ratio of monoisotopic extracted ion chromatograms of peptides containing the respective molecular species. α1(I) K918/K930 and other sites were analyzed using the collagenase/pepsin digests and the trypsin digests, respectively.

Masson's Trichrome stain – OHSU histology core facility performed sectioning and staining skin sample. Ventral skin tissues (n = 3) were fixed in 4% paraformaldehyde for 24 hours at 4°C. The fixed tissues were dehydrated using an ethanol gradient, cleared in xylene, and embedded in paraffin wax, after which 5 µm sections were cut using a microtome. The tissue sections were stained with Masson's

trichrome for collagen fiber analysis. Regions of interest (n = 2 - 4) were selected per image (n = 5) and thickness of dermis and hypodermis were measured. Length was normalized by each scale bar.

Electron Microscopy Analysis of skin – The three independently prepared skin from P3H3 null and WT mice was fixed in 1.5 % glutaraldehyde/1.5 % paraformaldehyde (Electron Microscopy Sciences) in Dulbecco's serum-free media (SFM) containing 0.05 % tannic acid. The samples were rinsed in SFM, post-fixed in 1 % OsO4 then dehydrated in a graded series of ethanol to 100 %, rinsed in propylene oxide and infiltrated in Spurr's epoxy. Samples were polymerized at 70 °C for 18 hours. Ultra-thin sections (~80 nm) were cut on a Leica EM UC7 ultramicrotome and mounted on formvar-coated, copper palladium 1x2 mm slot grids. Sections were stained in saturated uranyl acetate followed by lead citrate and photographed using an AMT 2K x 2K side entry camera (AMT, Woburn, MA) mounted on a FEI G2 transmission electron microscope operated at 120 kV and at least four images were taken per sample.

Fibril diameter measurement – The number and cross-sectional area of fibrils were measured using the Fiji software (ImageJ). Regions of interest were selected from the images of WT (n = 13) and P3H3 null (n = 17) and fibril areas were measured by counting the pixels per fibril, which accounts for μm^2. Spatial calibration for diameter measurements was applied against each scale bar. The numbers were counted as 1845 and 3616 fibrils for P3H3 WT and null.

Statistical analyses – For comparisons between two groups, we performed one-way ANOVA to determine whether differences between groups are significant using ORIGIN Pro ver. 9.1 (OriginLab Corp., Northampton, MA). The P value less than 0.05 was considered statistically significant.

References

1. Ricard-Blum S, Ruggiero F. The collagen superfamily: from the extracellular matrix to the cell membrane. Pathol Biol (Paris). 2005;53(7):430-42.
2. Bella J, Hulmes DJ. Fibrillar Collagens. Subcell Biochem. 2017;82:457-90.
3. Gjaltema RAF, Bank RA. Molecular insights into prolyl and lysyl hydroxylation of fibrillar collagens in health and disease. Critical Reviews in Biochemistry and Molecular Biology. 2018;52(1):74-95.
4. Yamauchi M, Shiiba M. Lysine hydroxylation and cross-linking of collagen. Methods Mol Biol. 2008;446:95-108.
5. Eyre DR, Paz MA, Gallop PM. Cross-linking in collagen and elastin. Annu Rev Biochem. 1984;53:717-48.
6. Yamauchi M, Sricholpech M. Lysine post-translational modifications of collagen. Essays Biochem. 2012;52:113-33.
7. Eyre DR, Weis MA, Wu JJ. Advances in collagen cross-link analysis. Methods. 2008;45(1):65-74.
8. Trackman PC. Enzymatic and non-enzymatic functions of the lysyl oxidase family in bone. Matrix Biol. 2016;52-54:7-18.
9. Wang C, Valtavaara M, Myllyla R. Lack of collagen type specificity for lysyl hydroxylase isoforms. DNA Cell Biol. 2000;19(2):71-7.
10. Marini JC, Cabral WA, Barnes AM. Null mutations in LEPRE1 and CRTAP cause severe recessive osteogenesis imperfecta. Cell Tissue Res. 2010;339(1):59-70.
11. Ishikawa Y, Boudko S, Bächinger H. Ziploc-ing the structure: Triple helix formation is coordinated by rough endoplasmic reticulum resident PPIases. Biochim Biophys Acta. 2015;1850(10):1983-93.
12. Hennet T. Collagen glycosylation. Curr Opin Struct Biol. 2019;56:131-8.
13. Ishikawa Y, Bächinger H. A molecular ensemble in the rER for procollagen maturation. Biochim Biophys Acta. 2013;1833(11):2479-91.
14. Berg RA, Prockop DJ. Purification of (14C) protocollagen and its hydroxylation by prolyl-hydroxylase. Biochemistry. 1973;12(18):3395-401.
15. Hieta R, Kukkola L, Permi P, Pirila P, Kivirikko KI, Kilpelainen I, et al. The peptide-substrate-binding domain of human collagen prolyl 4-hydroxylases. Backbone assignments, secondary structure, and binding of proline-rich peptides. J Biol Chem. 2003;278(37):34966-74.
16. Takaluoma K, Lantto J, Myllyharju J. Lysyl hydroxylase 2 is a specific telopeptide hydroxylase, while all three isoenzymes hydroxylate collagenous sequences. Matrix Biol. 2007;26(5):396-403.
17. Scietti L, Chiapparino A, De Giorgi F, Fumagalli M, Khoriauli L, Nergadze S, et al. Molecular architecture of the multifunctional collagen lysyl hydroxylase and glycosyltransferase LH3. Nat Commun. 2018;9(1):3163.
18. Hudson DM, Weis M, Rai J, Joeng KS, Dimori M, Lee BH, et al. P3h3-null and Sc65-null Mice Phenocopy the Collagen Lysine Under-hydroxylation and Cross-linking Abnormality of Ehlers-Danlos Syndrome Type VIA. J Biol Chem. 2017;292(9):3877-87.
19. Hyry M, Lantto J, Myllyharju J. Missense mutations that cause Bruck syndrome affect enzymatic activity, folding, and oligomerization of lysyl hydroxylase 2. J Biol Chem. 2009;284(45):30917-24.
20. Forlino A, Marini JC. Osteogenesis imperfecta. Lancet. 2016;387(10028):1657-71.
21. Malfait F. Vascular aspects of the Ehlers-Danlos Syndromes. Matrix Biol. 2018;71-72:380-95.
22. Risteli L, Risteli J, Ihme A, Krieg T, Muller PK. Preferential hydroxylation of type IV collagen by lysyl hydroxylase from Ehlers-Danlos syndrome type VI fibroblasts. Biochem Biophys Res Commun. 1980;96(4):1778-84.
23. Ihme A, Krieg T, Nerlich A, Feldmann U, Rauterberg J, Glanville RW, et al. Ehlers-Danlos syndrome type VI: collagen type specificity of defective lysyl hydroxylation in various tissues. J Invest Dermatol. 1984;83(3):161-5.

24. Ruotsalainen H, SipilÃ¤ L, Vapola M, Sormunen R, Salo AM, Uitto L, et al. Glycosylation catalyzed by lysyl hydroxylase 3 is essential for basement membranes. Journal of Cell Science. 2006;119(4):625-35.
25. Myllyla R, Wang C, Heikkinen J, Juffer A, Lampela O, Risteli M, et al. Expanding the lysyl hydroxylase toolbox: new insights into the localization and activities of lysyl hydroxylase 3 (LH3). J Cell Physiol. 2007;212(2):323-9.
26. Takaluoma K, Hyry M, Lantto J, Sormunen R, Bank RA, Kivirikko KI, et al. Tissue-specific changes in the hydroxylysine content and cross-links of collagens and alterations in fibril morphology in lysyl hydroxylase 1 knock-out mice. J Biol Chem. 2007;282(9):6588-96.
27. Van Dijk FS, Nesbitt IM, Nikkels PG, Dalton A, Bongers EM, van de Kamp JM, et al. CRTAP mutations in lethal and severe osteogenesis imperfecta: the importance of combining biochemical and molecular genetic analysis. Eur J Hum Genet. 2009;17(12):1560-9.
28. Mizuno K, Hayashi T, Bächinger H. Hydroxylation-induced stabilization of the collagen triple helix. Further characterization of peptides with 4(R)-hydroxyproline in the Xaa position. J Biol Chem. 2003;278(34):32373-9.
29. Kuznetsova NV, McBride DJ, Leikin S. Changes in thermal stability and microunfolding pattern of collagen helix resulting from the loss of alpha2(I) chain in osteogenesis imperfecta murine. J Mol Biol. 2003;331(1):191-200.
30. Pokidysheva E, Zientek KD, Ishikawa Y, Mizuno K, Vranka JA, Montgomery NT, et al. Posttranslational modifications in type I collagen from different tissues extracted from wild type and prolyl 3-hydroxylase 1 null mice. J Biol Chem. 2013;288(34):24742-52.
31. Terajima M, Taga Y, Chen Y, Cabral WA, Hou-Fu G, Srisawasdi S, et al. Cyclophilin-B Modulates Collagen Cross-linking by Differentially Affecting Lysine Hydroxylation in the Helical and Telopeptidyl Domains of Tendon Type I Collagen. J Biol Chem. 2016;291(18):9501-12.
32. Terajima M, Taga Y, Cabral WA, Liu Y, Nagasawa M, Sumida N, et al. Cyclophilin B control of lysine post-translational modifications of skin type I collagen. PLOS Genetics. 2019;15(6):e1008196.
33. Yang C, Park AC, Davis NA, Russell JD, Kim B, Brand DD, et al. Comprehensive mass spectrometric mapping of the hydroxylated amino acid residues of the alpha1(V) collagen chain. J Biol Chem. 2012;287(48):40598-610.
34. Wu GY, Pereyra B, Seifter S. Specificity of trypsin and carboxypeptidase B for hydroxylysine residues in denatured collagens. Biochemistry. 1981;20(15):4321-4.
35. Eyre DR, Wu J-J. Collagen Cross-Links. Springer Berlin Heidelberg; 2005. p. 207-29.
36. Exposito J-Y, Valcourt U, Cluzel C, Lethias C. The fibrillar collagen family. International journal of molecular sciences. 2010;11(2):407-26.
37. Hudson DM, Weis M, Eyre DR. Insights on the evolution of prolyl 3-hydroxylation sites from comparative analysis of chicken and Xenopus fibrillar collagens. PLoS One. 2011;6(5):e19336.
38. Ellgaard L, McCaul N, Chatsisvili A, Braakman I. Co- and Post-Translational Protein Folding in the ER. Traffic. 2016;17(6):615-38.
39. Kozlov G, Munoz-Escobar J, Castro K, Gehring K. Mapping the ER Interactome: The P Domains of Calnexin and Calreticulin as Plurivalent Adapters for Foldases and Chaperones. Structure. 2017;25(9):1415-22 e3.
40. DiChiara AS, Taylor RJ, Wong MY, Doan ND, Rosario AM, Shoulders MD. Mapping and Exploring the Collagen-I Proteostasis Network. ACS Chem Biol. 2016;11(5):1408-21.
41. Vranka JA, Sakai LY, Bächinger H. Prolyl 3-hydroxylase 1, enzyme characterization and identification of a novel family of enzymes. J Biol Chem. 2004;279(22):23615-21.
42. Wu J, Zhang W, Xia L, Feng L, Shu Z, Zhang J, et al. Characterization of PPIB interaction in the P3H1 ternary complex and implications for its pathological mutations. Cell Mol Life Sci. 2019;76(19):3899-914.
43. Choi JW, Sutor SL, Lindquist L, Evans GL, Madden BJ, Bergen HR, 3rd, et al. Severe osteogenesis imperfecta in cyclophilin B-deficient mice. PLoS Genet. 2009;5(12):e1000750.

528 44. Chang W, Barnes AM, Cabral WA, Bodurtha JN, Marini JC. Prolyl 3-hydroxylase 1 and CRTAP
529 are mutually stabilizing in the endoplasmic reticulum collagen prolyl 3-hydroxylation complex. Hum Mol
530 Genet. 2010;19(2):223-34.
531 45. Marini JC, Forlino A, Bächinger H, Bishop NJ, Byers PH, Paepe A, et al. Osteogenesis
532 imperfecta. Nat Rev Dis Primers. 2017;3:17052.
533 46. Ishikawa Y, Vranka JA, Boudko SP, Pokidysheva E, Mizuno K, Zientek K, et al. Mutation in
534 cyclophilin B that causes hyperelastosis cutis in American Quarter Horse does not affect peptidylprolyl
535 cis-trans isomerase activity but shows altered cyclophilin B-protein interactions and affects collagen
536 folding. J Biol Chem. 2012;287(26):22253-65.
537 47. Cabral WA, Perdivara I, Weis M, Terajima M, Blissett AR, Chang W, et al. Abnormal type I
538 collagen post-translational modification and crosslinking in a cyclophilin B KO mouse model of recessive
539 osteogenesis imperfecta. PLoS Genet. 2014;10(6):e1004465.
540 48. Heard ME, Besio R, Weis M, Rai J, Hudson DM, Dimori M, et al. Sc65-Null Mice Provide
541 Evidence for a Novel Endoplasmic Reticulum Complex Regulating Collagen Lysyl Hydroxylation. PLoS
542 Genet. 2016;12(4):e1006002.
543 49. Vranka JA, Pokidysheva E, Hayashi L, Zientek K, Mizuno K, Ishikawa Y, et al. Prolyl 3-
544 hydroxylase 1 null mice display abnormalities in fibrillar collagen-rich tissues such as tendons, skin, and
545 bones. J Biol Chem. 2010;285(22):17253-62.
546 50. Sweeney SM, Orgel JP, Fertala A, McAuliffe JD, Turner KR, Di Lullo GA, et al. Candidate cell
547 and matrix interaction domains on the collagen fibril, the predominant protein of vertebrates. J Biol Chem.
548 2008;283(30):21187-97.
549 51. Yeowell HN, Walker LC. Mutations in the lysyl hydroxylase 1 gene that result in enzyme
550 deficiency and the clinical phenotype of Ehlers-Danlos syndrome type VI. Mol Genet Metab. 2000;71(1-
551 2):212-24.
552 52. Taga Y, Kusubata M, Ogawa-Goto K, Hattori S. Stable isotope-labeled collagen: a novel and
553 versatile tool for quantitative collagen analyses using mass spectrometry. J Proteome Res.
554 2014;13(8):3671-8.
555 53. Koide T, Takahara Y, Asada S, Nagata K. Xaa-Arg-Gly triplets in the collagen triple helix are
556 dominant binding sites for the molecular chaperone HSP47. J Biol Chem. 2002;277(8):6178-82.
557

Acknowledgements

We thank to the Analytical Core Facility of Shriners Hospitals for Children in Portland for amino acid analysis and also to the OHSU histology core facility for sectioning and staining skin sample. We also thank Douglas B. Gould (Department of Ophthalmology, University of California, San Francisco) for critical reading of the manuscript and providing valuable comments. This study was supported by grants from Shriners Hospital for Children (85100 and 85500 to HPB) and by the Academy of Finland Project Grant 296498 and Center of Excellence 2012-2017 Grant 251314 (JM), the S. Jusélius Foundation (JM), and the Jane and Aatos Erkko Foundation (JM).

Author contributions

YI and HPB were responsible for the overall design of the study. YI, YT, KZ, NM, AS, OS, ST and DRK conducted and analyzed experiments. YI, YT, KZ, NM, AS, OS, ST, DRK, PH, KM, JM and HPB provided essential material, reviewed and discussed the results. YI and HPB wrote the main manuscript text. All authors were involved in editing the manuscript.

Additional information

Competing Interests: The authors declare that they have no competing interests related to this work.

Table 1: Comparison of overall proline and lysine post-translational modifications in type I collagen between tissues and type V collagen in skin.

			3Hyp (%)	P value	4Hyp (%)	P value	Pro (%)	P value	Lys (%)	P value	Hyl (%)	P value
col1	tendon	WT	0.95 ± 0.55	0.65658	44.5 ± 2.6	0.60898	54.6 ± 3.2	0.61666	80.3 ± 2.5	5.36786E-8	19.7 ± 2.5	5.36786E-8
		P3H3	1.06 ± 0.42		45.1 ± 2.2		53.8 ± 2.6		90.2 ± 0.9		9.8 ± 1.0	
		WT	1.14 ± 0.35	0.5239	47.3 ± 1.0	0.21519	51.7 ± 0.9	0.25603	81.1 ± 1.3	0	18.9 ± 1.3	0
		LH1	1.24 ± 0.39		46.7 ± 1.4		52.1 ± 1.2		98.4 ± 0.5		1.6 ± 0.5	
	skin	WT	0.32 ± 0.19	0.61795	46.6 ± 2.5	0.70334	53.1 ± 2.6	0.75642	86.5 ± 4.7	7.7608E-5	13.5 ± 4.7	7.7608E-5
		P3H3	0.37 ± 0.17		46.2 ± 2.5		53.4 ± 2.7		96.0 ± 1.3		4.0 ± 1.3	
		WT	0.52 ± 0.21	0.41975	51.1 ± 0.9	0.80229	48.4 ± 1.0	0.71858	81.2 ± 1.9	8.29004E-13	18.8 ± 1.9	8.29004E-13
		LH1	0.46 ± 0.09		51.0 ± 0.8		48.5 ± 0.8		98.1 ± 0.4		1.9 ± 0.4	
	bone	WT	1.46 ± 0.84	0.79823	48.1 ± 1.72	0.59762	50.5 ± 2.1	0.50736	78.0 ± 3.3	8.81801E-4	22.0 ± 3.3	8.81801E-4
		P3H3	1.28 ± 1.26		47.2 ± 2.9		51.7 ± 3.5		88.2 ± 3.0		11.8 ± 3.0	
		WT	0.85 ± 0.53	0.43429	48.0 ± 1.2	0.00101	51.1 ± 1.5	0.00811	84.0 ± 4.4	3.94453E-5	15.8 ± 4.3	3.04315E-5
		LH1	1.24 ± 0.87		43.1 ± 1.6		55.6 ± 2.2		96.7 ± 1.7		5.1 ± 1.6	
Col5	skin	WT	1.12 ± 1.06	0.84309	44.5 ± 3.0	0.99626	54.4 ± 3.2	0.94792	39.6 ± 4.7	7.65287E-5	60.4 ± 4.7	7.65284E-5
		P3H3	1.06 ± 0.77		44.5 ± 3.2		54.4 ± 2.9		48.6 ± 6.7		51.4 ± 6.7	
		WT	1.07 ± 0.20	0.1898	52.5 ± 2.1	0.05353	46.5 ± 2.3	0.03944	40.5 ± 2.6	0.41188	60.0 ± 2.6	0.41188
		LH1	2.03 ± 1.10		54.4 ± 0.5		43.5 ± 1.3		38.0 ± 4.2		62.0 ± 4.2	

Values are given as means ± S.D. Biological replicates were tendon: n ≥ 8, bone n ≥ 4, skin type I collagen: n = 8 and skin type V collagen: n ≥ 3.

3Hyp + 4Hyp + Pro = 100 % and Lys + Hyl = 100 %. Values of amino acids were obtained using amino acid analysis.

Note: 3Hyp; 3-hydroxyproline, 4Hyp; 4-hydroxyproline, Pro; unmodified proline, Lys; unmodified lysine, Hyl; hydroxylysine.

582 **Table 2. Occupancy (%) of glycosylation in total hydroxylysine residues**

			GGHL (%)	P-value	GHL (%)	P-value	Free Hyl (%)	P-value
Col1	tendon	WT	2.10 ± 0.05	1.50266E-4	1.84 ± 0.16	0.0033	96.1 ± 0.18	7.10419
		P3H3	5.38 ± 0.78		2.42 ± 0.19	7	92.2 ± 0.78	E-5
		WT	2.48 ± 0.25	3.69023E-4	2.00 ± 0.11	0.0028	95.5 ± 0.22	2.64133
		LH1	17.9 ± 4.28		3.15± 0.46	1	79.0 ± 4.33	E-4
	skin	WT	17.9 ± 1.34	0.01235	8.19 ± 0.51	0.9527	74.0 ±1.81	0.02079
		P3H3	14.2 ± 1.57		8.17 ± 0.52	9	77.6 ± 1.52	
		WT	17.2 ± 1.44	2.21409E-5	9.51± 0.77	0.6023	73.3 ± 0.80	4.36518
		LH1	7.74 ± 0.72		9.16 ± 1.02	3	83.1 ±1.70	E-5
Col5	skin	WT	84.0 ± 0.77	0.58681	3.45 ± 0.11	0.0678	12.6 ± 0.71	0.81673
		P3H3	83.7 ± 0.64		3.66 ± 0.10	1	12.7 ± 0.57	

583 Values are given as means ± S.D. ($n \geq 3$). Biological replicates were n = 4 for all tissues and genotypes.

584 Free Hyl + GHL + GGHL = 100 %. Values of glycosylated hydroxylines and unmodified hydroxylysine
585 were obtained using mass spectrometry.

586 Note: Free Hyl; unmodified hydroxylysine, GHL; galactosyl hydroxylysine, GGHL; glucosylgalactosyl
587 hydroxylysine

Table 3: Comparison of lysine post-translational modifications of tendon type I collagen at individual sites.

			Lys (%)	P value	Hyl (%)	P value	GHL (%)	P value	GGHL (%)	P value
α1 K87	P3H3	WT	0.56 ± 0.17	3.91E-10	96.8 ± 0.26	4.19E-10	1.70 ± 0.07	4.84E-07	0.93 ± 0.02	7.49E-07
		Null	49.1 ± 1.29		49.7 ± 1.25		0.77 ± 0.04		0.46 ± 0.04	
	LH1	WT	4.03 ± 1.86	5.84E-11	93.1 ± 1.85	6.77E-11	1.76 ± 0.02	1.70E-11	1.10 ± 0.02	1.12E-09
		Null	99.4 ± 0.13		0.45 ± 0.11		0.04 ± 0.01		0.12 ± 0.02	
α2 K87	P3H3	WT	0.35 ± 0.04	6.42E-12	99.7 ± 0.04	6.42E-12	ND		ND	
		Null	36.9 ± 0.49		63.1 ± 0.49		ND		ND	
	LH1	WT	0.30 ± 0.07	0	99.7 ± 0.07	0	ND		ND	
		Null	99.3 ± 0.12		0.66 ± 0.12		ND		ND	
α1 K99	P3H3	WT	76.8 ± 0.48	8.47E-09	18.6 ± 0.47	1.18E-08	1.47 ± 0.02	5.96E-10	0.10 ± 0.01	1.02E-04
		Null	92.8 ± 0.33		6.53 ± 0.33		0.60 ± 0.01		0.05 ± 0.01	
	LH1	WT	79.7 ± 0.56	7.94E-10	18.6 ± 0.53	1.05E-09	1.59 ± 0.08	2.31E-08	0.12 ± 0.01	1.33E-06
		Null	99.1 ± 0.18		0.80 ± 0.17		0.08 ± 0.07		0	
α1 K174	P3H3	WT	60.5 ± 1.20	3.13E-05	38.8 ± 1.18	3.43E-05	0.71 ± 0.03	2.22E-04	ND	
		Null	67.7 ± 0.51		31.7 ± 0.54		0.53 ± 0.03		ND	
	LH1	WT	59.5 ± 1.31	1.53E-08	39.8 ± 1.31	1.81E-08	0.76 ± 0.05	6.70E-08	ND	
		Null	86.8 ± 0.32		13.2 ± 0.32		0		ND	
α2 K174	P3H3	WT	15.2 ± 0.26	2.95E-12	82.2 ± 0.17	2.90E-12	2.53 ± 0.10	8.17E-09	0.06 ± 0.01	7.01E-05
		Null	81.6 ± 0.74		18.2 ± 0.74		0.22 ± 0.03		0	
	LH1	WT	11.6 ± 0.57	7.91E-12	85.3 ± 0.40	6.56E-12	3.02 ± 0.21	1.15E-07	0.05 ± 0.01	2.56E-04
		Null	92.1 ± 0.97		7.92 ± 0.97		0		0	
α1 K219	P3H3	WT	73.1 ± 1.10	0.6388	26.9 ± 1.10	0.6388	ND		ND	
		Null	72.7 ± 1.07		27.3 ± 1.07		ND		ND	
	LH1	WT	75.9 ± 1.16	2.90E-07	24.1 ± 1.16	2.90E-07	ND		ND	
		Null	92.7 ± 0.71		7.28 ± 0.71		ND		ND	
α2 K219	P3H3	WT	51.6 ± 0.51	4.67E-08	30.5 ± 0.54	0.00259	17.1 ± 0.16	1.02E-11	0.84 ± 0.02	5.20E-09
		Null	64.1 ± 0.54		32.5 ± 0.62		3.27 ± 0.12		0.14 ± 0.02	
	LH1	WT	48.3 ± 1.30	5.04E-08	31.4 ± 1.19	2.65E-06	19.2 ± 0.06	2.61E-14	1.09 ± 0.07	4.93E-08
		Null	87.1 ± 1.94		12.6 ± 1.86		0.38 ± 0.08		0	
α1 K564	P3H3	WT	79.1 ± 1.09	0.01211	20.1 ± 1.05	0.01518	0.63 ± 0.04	0.00221	0.19 ± 0.01	1.12E-04
		Null	76.7 ± 0.81		22.3 ± 0.79		0.77 ± 0.03		0.27 ± 0.01	
	LH1	WT	80.1 ± 1.61	1.05E-06	18.8 ± 1.57	1.15E-06	0.66 ± 0.05	4.86E-07	0.22 ± 0.02	1.83E-04
		Null	96.5 ± 0.19		3.30 ± 0.19		0.06 ± 0.01		0.14 ± 0.01	
α2 K933	P3H3	WT	0.99 ± 0.12	2.22E-16	93.7 ± 1.15	9.40E-12	5.34 ± 1.20	2.84E-04	ND	
		Null	85.6 ± 0.16		13.6 ± 0.13		0.81 ± 0.08		ND	
	LH1	WT	0.52 ± 0.05	0	91.6 ± 0.45	2.04E-14	7.92 ± 0.48	5.00E-08	ND	
		Null	99.2 ± 0.12		0.75 ± 0.12		0		ND	

			Lys-Lys (%)	P value	Lys-Hyl (%)	P value	Hyl-Hyl (%)	P value
α1 K918/K930	P3H3	WT	11.3 ± 0.29	1.14E-06	12.7 ± 0.58	0.13635	76.0 ± 0.75	5.17E-10
		Null	90.5 ± 8.07		7.43 ± 6.15		2.05 ± 1.94	
	LH1	WT	7.63 ± 0.41	3.32E-13	11.3 ± 0.41	3.26E-09	81.0 ± 0.75	3.06E-12
		Null	99.2 ± 0.63		0.30 ± 0.08		0.51 ± 0.60	

Values are given as means ± S.D. (n ≥ 3). Biological replicates were n = 4 for all tissues and genotypes.

590 Lys + Hyl + GHL + GGHL = 100 % and Lys-Lys + Lys-Hyl + Hyl-Hyl = 100 %. Values of modified and unmodified hydroxylines and unmodified lysine and
591 were obtained using mass spectrometry. Note: Lys; unmodified lysine, Hyl; unmodified hydroxylysine, GHL; galactosyl hydroxylysine, GGHL;
592 glucosylgalactosyl hydroxylysine, Lys-Lys; unmodified lysine and unmodified lysine, Lys-Hyl; unmodified lysine and unmodified hydroxylysine, Hyl-Hyl;
593 unmodified hydroxylysine and unmodified hydroxylysine

Table 4: Comparison of lysine post-translational modifications of skin type I collagen at individual sites.

			Lys (%)	P value	Hyl (%)	P value	GHL (%)	P value	GGHL (%)	P value
α1 K87	P3H3	WT	15.7 ± 13.3	9.78E-05	2.35 ± 0.24	1.01E-05	7.35 ± 1.08	1.03E-04	74.6 ± 12.3	4.49E-05
		Null	77.8 ± 3.06		10.3 ± 1.15		2.30 ± 0.28		9.65 ± 1.78	
	LH1	WT	8.28 ± 5.34	4.34E-08	2.06 ± 0.37	1.59E-04	6.83 ± 0.36	2.77E-08	82.8 ± 5.18	6.40E-08
		Null	98.9 ± 0.12		0.47 ± 0.78		0.20 ± 0.01		0.42 ± 0.03	
α2 K87	P3H3	WT	6.41 ± 3.13	2.95E-08	93.6 ± 3.13	2.95E-08	ND		ND	
		Null	73.0 ± 1.92		27.0 ± 1.92		ND		ND	
	LH1	WT	2.40 ± 0.28	3.33E-15	97.6 ± 0.28	3.33E-15	ND		ND	
		Null	98.0 ± 0.24		2.04 ± 0.24		ND		ND	
α1 K99	P3H3	WT	76.5 ± 2.31	3.83E-05	20.4 ± 1.43	1.27E-05	2.86 ± 0.91	0.00916	0.32 ± 0.11	0.08426
		Null	91.0 ± 1.40		7.68 ± 1.31		1.11 ± 0.12		0.19 ± 0.06	
	LH1	WT	78.4 ± 0.82	1.21E-08	17.5 ± 1.06	1.46E-07	3.54 ± 0.23	4.29E-07	0.62 ± 0.05	9.04E-06
		Null	96.5 ± 0.26		2.70 ± 0.13		0.64 ± 0.11		0.18 ± 0.03	
α1 K174	P3H3	WT	66.7 ± 4.73	3.38E-04	32.2 ± 4.34	2.82E-04	1.16 ± 0.44	0.00656	0	0
		Null	84.2 ± 0.84		15.5 ± 0.79		0.24 ± 0.10		0	
	LH1	WT	63.1 ± 0.50	3.00E-11	34.4 ± 0.50	5.13E-11	1.88 ± 0.06	9.56E-09	0.53 ± 0.02	9.22E-09
		Null	92.1 ± 0.07		7.69 ± 0.11		0.24 ± 0.04		0	
α2 K174	P3H3	WT	40.6 ± 13.1	2.16E-04	4.86 ± 1.24	0.48365	50.6 ± 10.6	9.59E-05	3.94 ± 1.76	0.00418
		Null	92.6 ± 1.27		5.40 ± 0.73		2.00 ± 1.21		0	
	LH1	WT	22.7 ± 1.17	4.31E-11	7.89 ± 0.80	3.12E-04	60.0 ± 0.79	9.10E-12	9.47 ± 0.48	2.07E-08
		Null	92.9 ± 0.58		4.59 ± 0.39		2.35 ± 0.23		0.20 ± 0.02	
α1 K219	P3H3	WT	86.2 ± 1.55	0.00779	13.8 ± 1.55	0.00779	ND		ND	
		Null	90.0 ± 1.11		10.0 ± 1.11		ND		ND	
	LH1	WT	85.3 ± 0.48	1.67E-07	14.7 ± 0.48	1.67E-07	ND		ND	
		Null	95.1 ± 0.54		4.91 ± 0.54		ND		ND	
α2 K219	P3H3	WT	55.1 ± 7.05	0.00133	34.0 ± 4.12	0.0033	0.62 ± 0.21	0.00161	10.3 ± 2.77	5.15E-04
		Null	75.2 ± 0.91		23.9 ± 1.09		0.03 ± 0.04		0.88 ± 0.25	
	LH1	WT	50.3 ± 0.79	6.51E-10	34.7 ± 0.92	2.31E-08	0.91 ± 0.13	1.70E-05	13.9 ± 0.63	1.42E-08
		Null	85.4 ± 0.65		13.7 ± 0.64		0.08 ± 0.02		0.80 ± 0.09	
α1 K564	P3H3	WT	77.3 ± 1.20	0.7026	20.3 ± 1.06	0.33603	1.72 ± 0.13	0.07732	0.70 ± 0.12	0.13392
		Null	77.6 ± 0.79		19.7 ± 0.65		1.93 ± 0.14		0.85 ± 0.13	
	LH1	WT	78.9 ± 0.82	1.20E-07	18.4 ± 0.58	4.12E-08	2.00 ± 0.19	7.87E-06	0.69 ± 0.10	3.30E-04
		Null	92.4 ± 0.47		6.76 ± 0.35		0.55 ± 0.07		0.28 ± 0.05	
α2 K933	P3H3	WT	0	3.58E-11	93.1 ± 0.37	2.12E-09	6.86 ± 2.37	0.00117	ND	
		Null	86.7 ± 1.56		13.3 ± 1.56		0		ND	
	LH1	WT	0	5.55E-16	93.0 ± 1.23	7.36E-12	7.02 ± 1.23	2.65E-05	ND	
		Null	97.9 ± 0.28		2.05 ± 0.28		0		ND	

			Lys-Lys (%)	P value	Lys-Hyl (%)	P value	Hyl-Hyl (%)	P value
α1 K918/K930	P3H3	WT	1.57 ± 0.73	5.07E-07	8.11 ± 2.66	0.09689	90.3 ± 3.17	3.67E-07
		Null	88.9 ± 7.73		5.16 ± 1.41		5.99 ± 6.36	
	LH1	WT	0.29 ± 0.21	1.11E-16	4.00 ± 0.18	4.47E-08	95.7 ± 0.21	3.33E-16
		Null	99.0 ± 0.06		0.78 ± 0.07		0.22 ± 0.12	

Values are given as means ± S.D. Biological replicates were n = 4 for all tissues and genotypes.

Lys + Hyl + GHL + GGHL = 100 % and Lys-Lys + Lys-Hyl + Hyl-Hyl = 100 %. Values of modified and unmodified hydroxylines and unmodified lysine and were obtained using mass spectrometry. Note: Lys; unmodified lysine, Hyl; unmodified hydroxylysine, GHL; galactosyl hydroxylysine, GGHL; glucosylgalactosyl hydroxylysine, Lys-Lys; unmodified lysine and unmodified lysine, Lys-Hyl; unmodified lysine and unmodified hydroxylysine, Hyl-Hyl; unmodified hydroxylysine and unmodified hydroxylysine

600 **Table 5: Comparison of lysine post-translational modifications of skin type V collagen in individual sites.**

			Lys (%)	P value	Hyl (%)	P value	GHL (%)	P value	GGHL (%)	P value
α1 K84	P3H3	WT	0.63 ± 0.04	0.06323	2.97 ± 0.09	0.05873	6.61 ± 0.37	0.23762	89.8 ± 0.36	0.05822
		Null	12.3 ± 7.94		3.95 ± 0.65		6.01 ± 0.56		77.6 ± 8.01	
	LH1	WT	1.33 ± 0.92	0.05917	2.28 ± 0.48	0.92243	6.56 ± 0.17	0.06623	89.9 ± 0.66	0.01655
		Null	3.25 ± 1.38		2.30 ± 0.12		6.88 ± 0.21		87.6 ± 1.18	
α2 K87	P3H3	WT	0	0.02794	16.2 ± 1.95	0.17434	4.55 ± 0.22	0.26084	79.3 ± 1.88	0.0248
		Null	8.07 ± 4.14		18.6 ± 1.59		4.55 ± 0.17		69.0 ± 4.71	
	LH1	WT	7.87 ± 8.46	0.00938	7.13 ± 1.51	0.61402	5.07 ± 0.65	0.01839	79.9 ± 7.92	0.00827
		Null	37.3 ± 1.00		6.68 ± 0.74		3.33 ± 0.67		52.7 ± 8.79	

601 Values are given as means ± S.D. Biological replicates were n =3 for P3H3 WT and null, n ≥ 3 for LH1 WT and n = 4 for LH1 null.

602 Lys + Hyl + GHL + GGHL = 100 %. Values of modified and unmodified hydroxylines and unmodified lysine were obtained using mass
603 spectrometry.

604 Note: Lys; unmodified lysine, Hyl; unmodified hydroxylysine, GHL; galactosyl hydroxylysine, GGHL; glucosylgalactosyl hydroxylysine

605 **Figure Legends**

606

607 **Figure 1. Generation of P3H3 null mice.** (A) Strategy for generation of the P3H3 null mice.
608 The mouse *Leprel2* gene was eliminated using FRT sites and loxP sites by an FLPe recombinase
609 followed by a Cre recombinase in ES cell, respectively. (B) PCR genotyping of P3H3 wild type
610 (WT), heterozygote (Het) and homozygote (Null) mice and smaller PCR products were
611 generated in Het and Null due to deletion of Exon 1. (C) Total soluble proteins from 3-month-
612 old whole mouse kidney in P3H3 WT, Het and Null were extracted and blotted by using anti-
613 GAPDH and anti-P3H3. The asterisk and black line in the panel of P3H3 indicate the band of
614 P3H3 and non-specific bands generated by antibodies, respectively. (D) Whole body weights of
615 P3H3 WT and Het male (red) and female (green) and P3H3 Null male (blue) and female
616 (magenta) were plotted as a function of age with standard deviations. Growth differences were
617 not observed. (E) Full body x-rays of 4-month-old female P3H3 WT and Null were scanned
618 from top and side angles. No skeletal defects were found.

619

620 **Figure 2. Biochemical characterization of type I collagen from P3H3 and LH1 Null mice.**
621 (A: upper panel) SDS-PAGE analysis of purified pepsin treated type I collagen of P3H3 WT and
622 null from skin, tendon and bone. Figure shows the final purified material in the presence of
623 reducing agent running on a NuPAGE 3 – 8 % Tris-Acetate gel (ThermoFisher) stained with
624 GelCode Blue Stain Reagent (ThermoFisher). (A: lower panel) Thermal stability of type I
625 collagen of P3H3 WT (blue) and null (red) from skin, tendon and bone were monitored by CD at
626 221 nm in 0.05 M acetic acid at 10 °C/h heating rate. P3H3 indicates P3H3 null and tissues were
627 collected from 2~5-month-old mice. Biological replicates of each curve were n = 3 for skin
628 P3H3 null, tendon P3H3 WT and null, n = 4 for skin P3H3 WT and bone P3H3 WT and n = 5
629 for bone P3H3 null. (B: upper panel) SDS-PAGE analysis of purified pepsin treated type I
630 collagen of LH1 WT and null from skin, tendon and bone. Figure shows the final purified
631 material in the presence of reducing agent running on a NuPAGE 3 – 8 % Tris-Acetate gel
632 (ThermoFisher) stained with GelCode Blue Stain Reagent. (B: lower panel) Thermal stability of
633 type I collagen of LH1 WT (blue) and null (red) from skin, tendon and bone were monitored by
634 CD at 221 nm in 0.05 M acetic acid at 10 °C/h heating rate. LH1 indicates LH1 null and tissues
635 were collected from 10-week-old mice. Biological replicates of each curve were n = 4 for all

636 tissues and genotypes. For both SDS-PAGE analysis of P3H3 and LH1, each genotype had three
637 biological replicates since each lane in gel was loaded by independently prepared collagen from
638 tissue.
639
640 **Figure 3. Summary of overall proline and lysine post-translational modifications in type I**
641 **collagen between tissues.** The ratio of post-translational modifications in proline (3Hyp + 4Hyp
642 + Pro = 100) and lysine (Lys + Hyl = 100) in type I collagen of WTs, P3H3 null and LH1 null
643 from tendon, skin and bone are demonstrated as bar graphs which are generated by values from
644 Table 1. Values of amino acids were obtained using amino acid analysis and biological
645 replicates were tendon: $n \geq 8$, skin: $n = 8$ and bone $n \geq 4$. The numbers in the graphs indicate the
646 mean ± S.D. of individual amino acids and P values obtained by statistical analyses are in Table
647 1 [3Hyp(magenta); 3-hydroxyproline, 4Hyp (cyan); 4-hydroxyproline, Pro (yellow); unmodified
648 proline, Lys (green); unmodified lysine, Hyl (blue); hydroxylysine]. P3H3 and LH1 indicate
649 P3H3 null and LH1 null, respectively.
650
651 **Figure 4. Summary of overall occupancy of *O*-glycosylation attached to hydroxylysine in**
652 **type I collagen between tissues.** The occupancy of *O*-glycosylation attached to hydroxylysine
653 (GGHL + GHL + Free Hyl = 100) in type I collagen of WTs, P3H3 null and LH1 null from
654 tendon and skin are demonstrated as bar graphs which are generated by values from Table 2.
655 Values of *O*-glycosylation and unmodified hydroxylysine were obtained by LC–MS after
656 alkaline hydrolysis and biological replicates were $n = 4$ for all tissues and genotypes. The
657 numbers in the graphs indicate the mean ± S.D. of individual *O*-glycosylation and unmodified
658 hydroxylysine and P values obtained by statistical analyses are in Table 2 [GGHL (gray);
659 glucosylgalactosyl hydroxylysine, GHL (light pink); galactosyl hydroxylysine, Free Hyl (dark
660 pink); unmodified hydroxylysine]. In figure, P3H3 and LH1 indicate P3H3 null and LH1 null,
661 respectively.
662
663 **Figure 5. Summary of lysine post-translational modifications of tendon type I collagen in**
664 **individual sites.** Bar graphs represent the occupancy of lysine modifications in individual lysyl
665 hydroxylation sites of type I collagen of WTs, P3H3 null and LH1 from tendon and skin.
666 Individual values [GGHL (cyan); glucosylgalactosyl hydroxylysine, GHL (magenta); galactosyl

667 hydroxylysine, Hyl (yellow); unmodified hydroxylysine, Lys (green); unmodified lysine, Hyl-
668 Hyl (dark cyan); unmodified hydroxylysine and unmodified hydroxylysine, Lys-Hyl (purple);
669 unmodified lysine and unmodified hydroxylysine, Lys-Lys (orange); unmodified lysine and
670 unmodified lysine] correspond to Table 3 and Table 4 for tendon and skin, respectively. Values
671 of modified and unmodified hydroxylines and unmodified lysine were obtained using mass
672 spectrometry and biological replicates were n = 4 for all tissues and genotypes. α1, α2 and K +
673 numbers indicate α1 and α2 chain of type I collagen and residue number from the first residue of
674 triple helical domain.
675
676 **Figure 6. Characterization of skin type V collagen from P3H3 and LH1 null mice.** (A)
677 SDS-PAGE analysis of purified pepsin treated skin type V collagen of WTs, P3H3 and LH1 null
678 mice. The final purified material in the presence of reducing agent was run running on a
679 NuPAGE 3 – 8 % Tris-Acetate gel stained with GelCode Blue Stain Reagent. For both SDS-
680 PAGE analysis of P3H3 and LH1, each genotype had three biological replicates since each lane
681 in gel was loaded by independently prepared collagen from tissue. (B) The ratio of post-
682 translational modifications in proline (3Hyp + 4Hyp + Pro = 100) and lysine (Lys + Hyl = 100)
683 in skin type V collagen of WTs, P3H3 null and LH1 null are demonstrated as bar graphs which
684 are generated by values from Table 1. Values of amino acids were obtained using amino acid
685 analysis and biological replicates were n = 17 for P3H3, n = 3 for LH1 WT and n = 6 for LH1
686 null. The numbers in the graphs indicate the mean ± S.D. of individual amino acids and P values
687 obtained by statistical analyses are in Table 1 [3Hyp(magenta); 3-hydroxyproline, 4Hyp (cyan);
688 4-hydroxyproline n, Pro (yellow); unmodified proline, Lys (green); unmodified lysine, Hyl
689 (blue); hydroxylysine]. (C) Thermal stability of skin type V collagen from P3H3 WT (blue) and
690 null (red) was monitored by CD at 221 nm in 0.05 M acetic acid, and the rate of heating was
691 10 °C/h. Biological replicates of each curve were n = 2 for both WT and P3H3 null. In figures,
692 P3H3 and LH1 indicate P3H3 null and LH1 null, respectively. Tissues were collected from 2~5-
693 month-old mice.
694
695 **Figure 7. Summary of lysine post-translational modifications of skin type V collagen in**
696 **individual sites.** Bar graphs represent the occupancy of lysine modifications in individual lysyl
697 hydroxylation sites of skin type V collagen of WTs, P3H3 null and LH1. Individual values

[GGHL (cyan); glucosylgalactosyl hydroxylysine, GHL (magenta); galactosyl hydroxylysine, Hyl (yellow); unmodified hydroxylysine, Lys (green); unmodified lysine] correspond to Table 5. Values of modified and unmodified hydroxylysines and unmodified lysine were obtained using mass spectrometry and biological replicates were n =3 for P3H3 WT and null, n ≥ 3 for LH1 WT and n = 4 for LH1 null. α1, α2 and K + numbers indicate that α1 and α2 chain of type V collagen and residue number from the first residue of triple helical domain.

Figure 8. Skin analysis of P3H3 null mice. (A) Masson's Trichrome stain was performed using skin section from 8-month-old P3H3 WT and null mice. D and H indicate dermis and hypodermis corresponding to the blue rich and white rich area, respectively. Scale bars, 200 μm. (B) The thickness of dermis and hypodermis were measured from the images of Masson's Trichrome stains. The averaged thickness of dermis and hypodermis are 350.6 ± 78.2 μm and 137.1 ± 28.7 μm for WT and 275.0 ± 80.1 μm and 335.7 ± 48.6 μm for P3H3 null. * and *** indicate $P < 0.05$ ($P = 0.013$) and $P < 0.0005$ ($P = 1.4988E^{-14}$), respectively. (C) The ratio between dermis and hypodermis was calculated by the set of thickness including both dermis and hypodermis from Masson's Trichrome stains. The averaged ratio between dermis and hypodermis are 2.64 ± 0.73 for WT and 0.84 ± 0.30 for P3H3 null. *** indicate $P < 0.0005$ as $P = 1.96408E^{-9}$. (D) Electron microscopy images display the skin collagen fibrils in 3-month-old P3H3 WT and null mice. Scale bar, 500 nm. (E) The histogram represents the fibril diameter distribution in P3H3 WT (cyan) and null (magenta). The averaged fibril diameter of P3H3 null and WT are 84.9 ± 35.6 nm and 85.1 ± 25.9 nm, respectively. The thickness of collagen fibrils was counted using electron microscopy images.

Figure 9. The magnitudes of change of unmodified lysine residues in individual lysyl hydroxylation sites of type I collagen between null mice models compared to WT. Schematic diagram and heat map show the magnitudes of change of unmodified lysine residues in individual lysyl hydroxylation sites. This change was calculated by [the value of unmodified lysine (%) in null mice] – [the value of unmodified lysine (%) in WT mice]. The values in Tables 3 and 4 were used for P3H3 null and LH1 null mice to calculate the changes. The values of unmodified lysine were obtained from reference [31] and [32] for CypB null mice in tendon and skin, respectively.

729

730 **Figure 10. The sequence alignment surrounding lysyl hydroxylation sites in type I and type**
731 **V collagen between human, mouse and bovine.** The sequences are aligned ± 12 residues from
732 the lysine residue which is modified to hydroxylysine and highlighted by yellow with Bold.
733 Glycine residues in GXY repeats and the residues not conserved between human, mouse and
734 bovine are highlighted by cyan and green. Arginine residues in RGXY sequences are also
735 highlighted by magenta because these residues are critical for Hsp47 to bind to collagen triple
736 helices [53]. Uniprot entry numbers are as follows: human COL1A1 (P02452), mouse COL1A1
737 (P11087), bovine COL1A1 (P02453), human COL1A2 (P08123), mouse COL1A2 (Q01149),
738 bovine COL1A2 (P02465), human COL5A1 (P20908), mouse COL5A1 (O88207), human
739 COL5A2 (P05997) and mouse COL5A2 (Q3U962). NCBI accession numbers are follows:
740 bovine COL5A1 (XP_024855494) and bovine COL5A2 (XP_024835542)

741

Figure 1

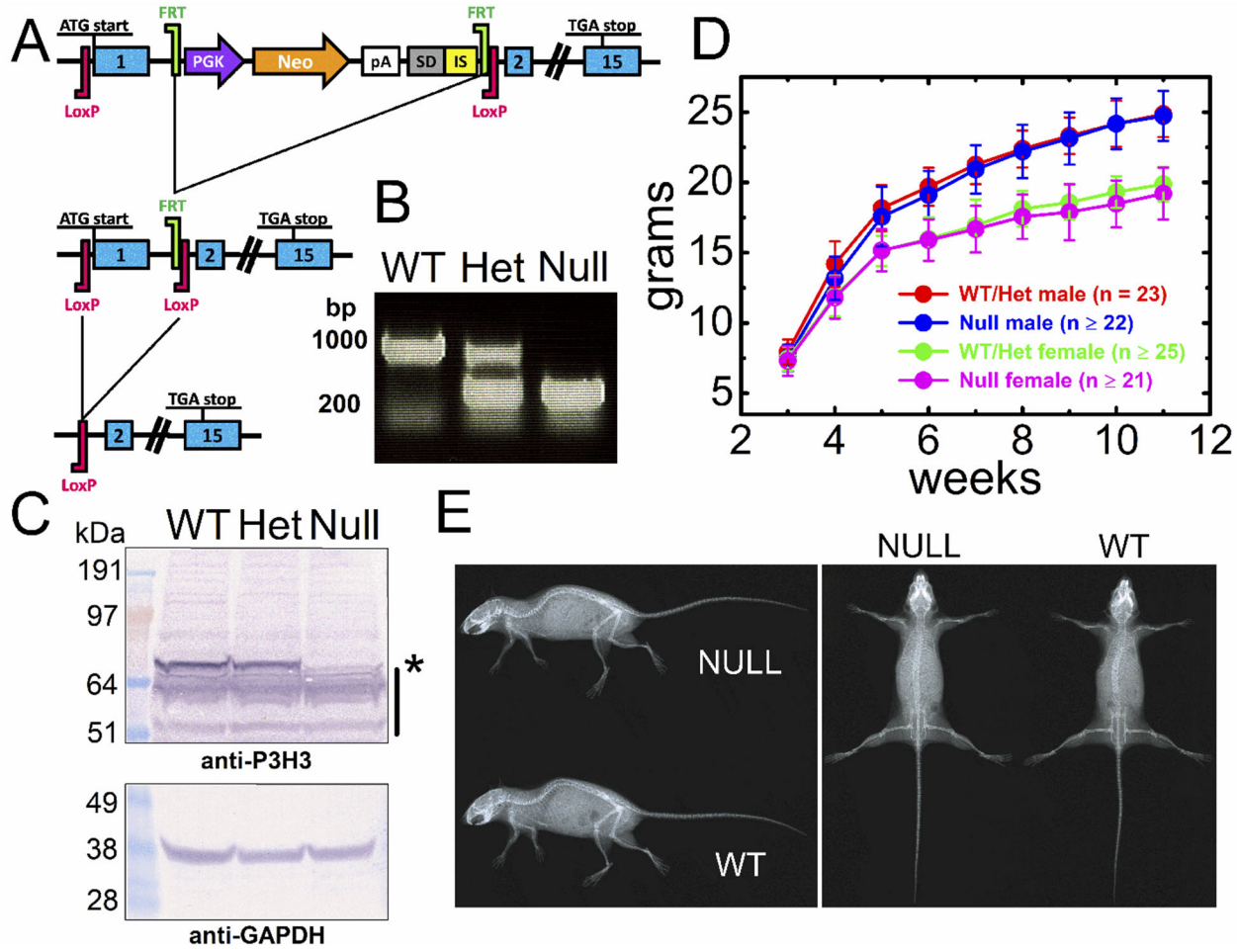

745 **Figure 2**

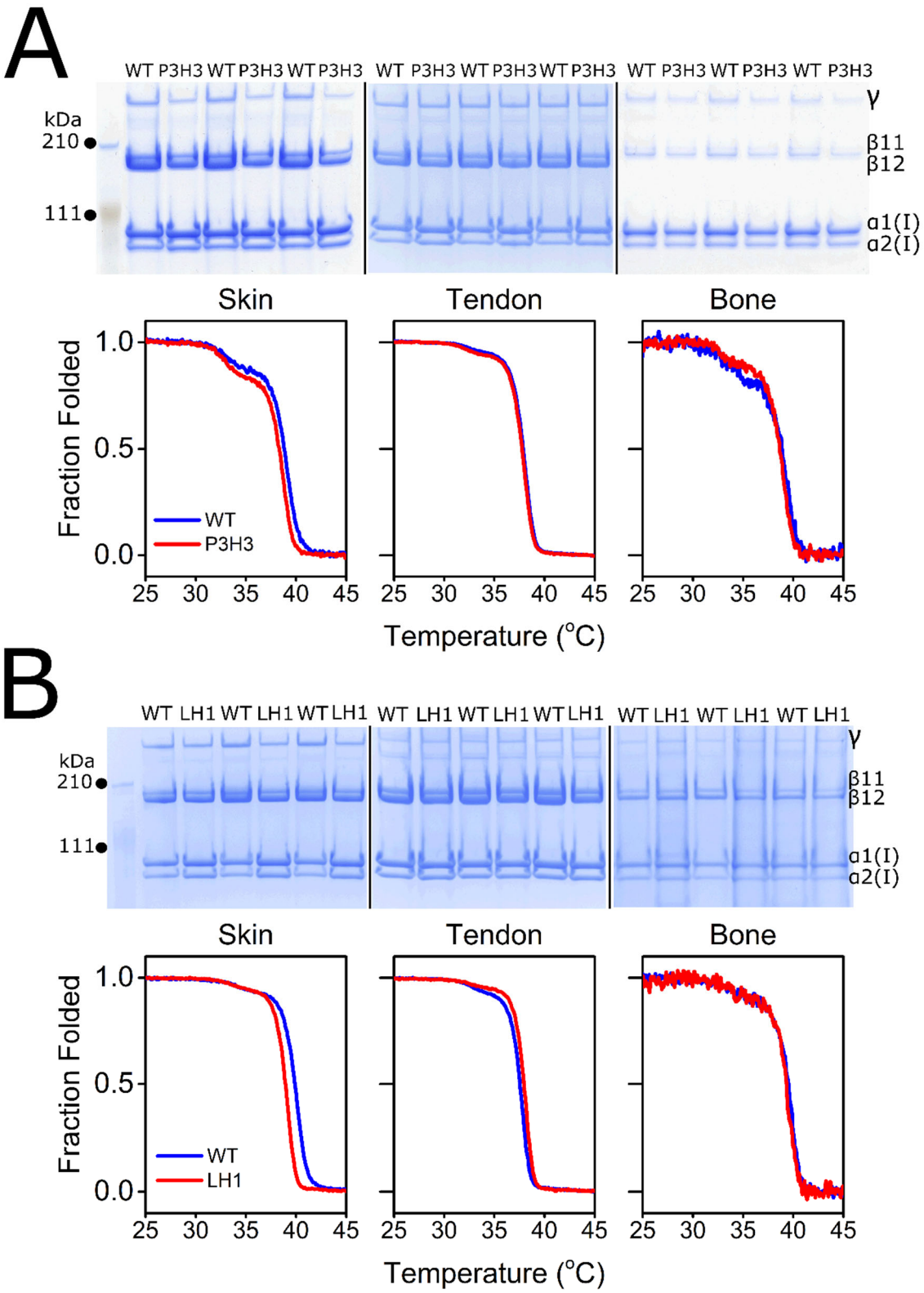

746

747

748 **Figure 3**

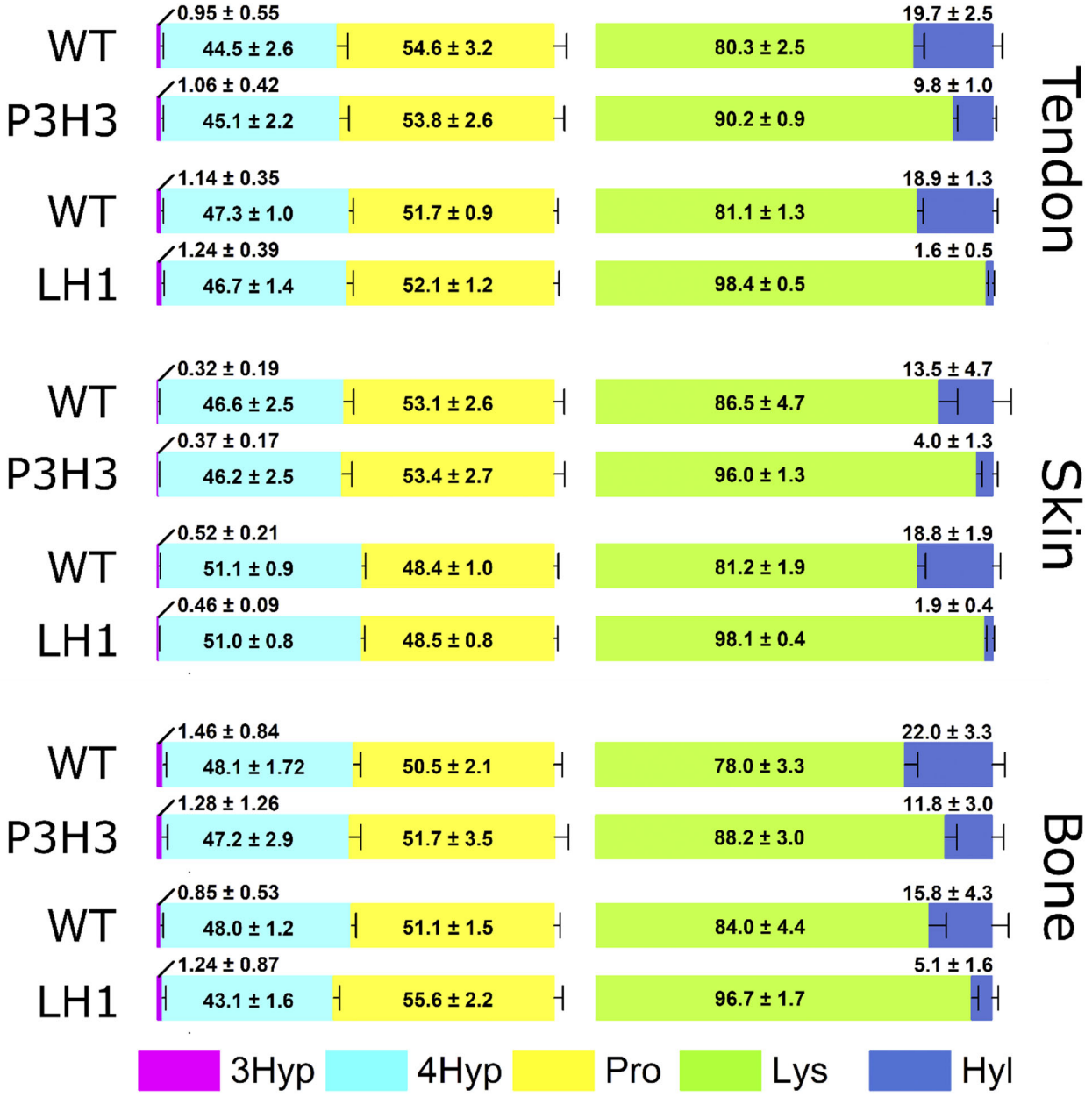

749

750

751 **Figure 4**

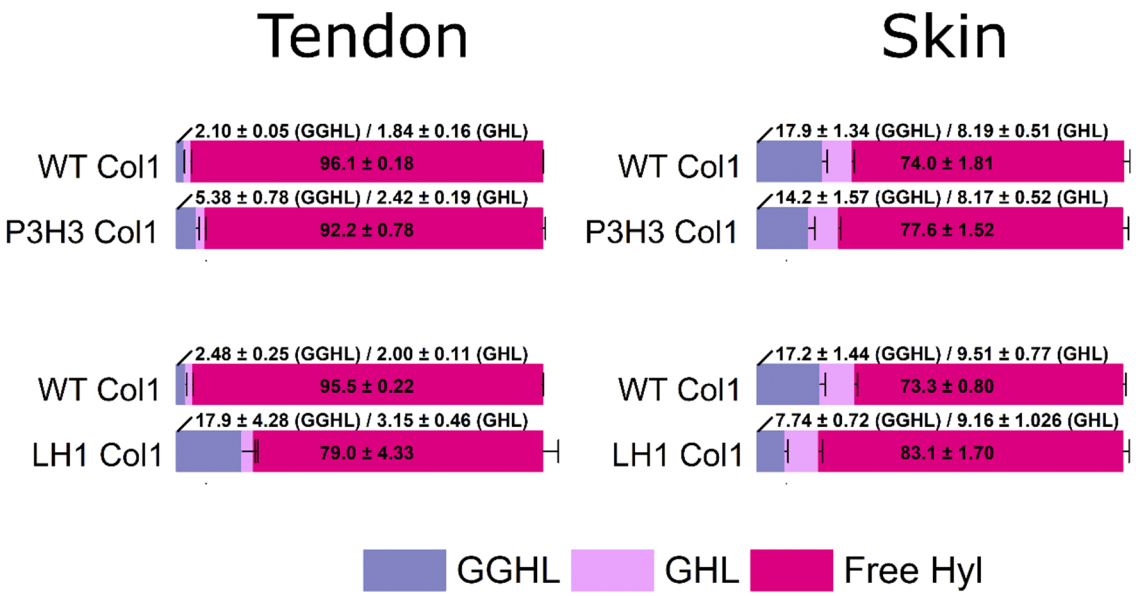

752

753

754 **Figure 5**

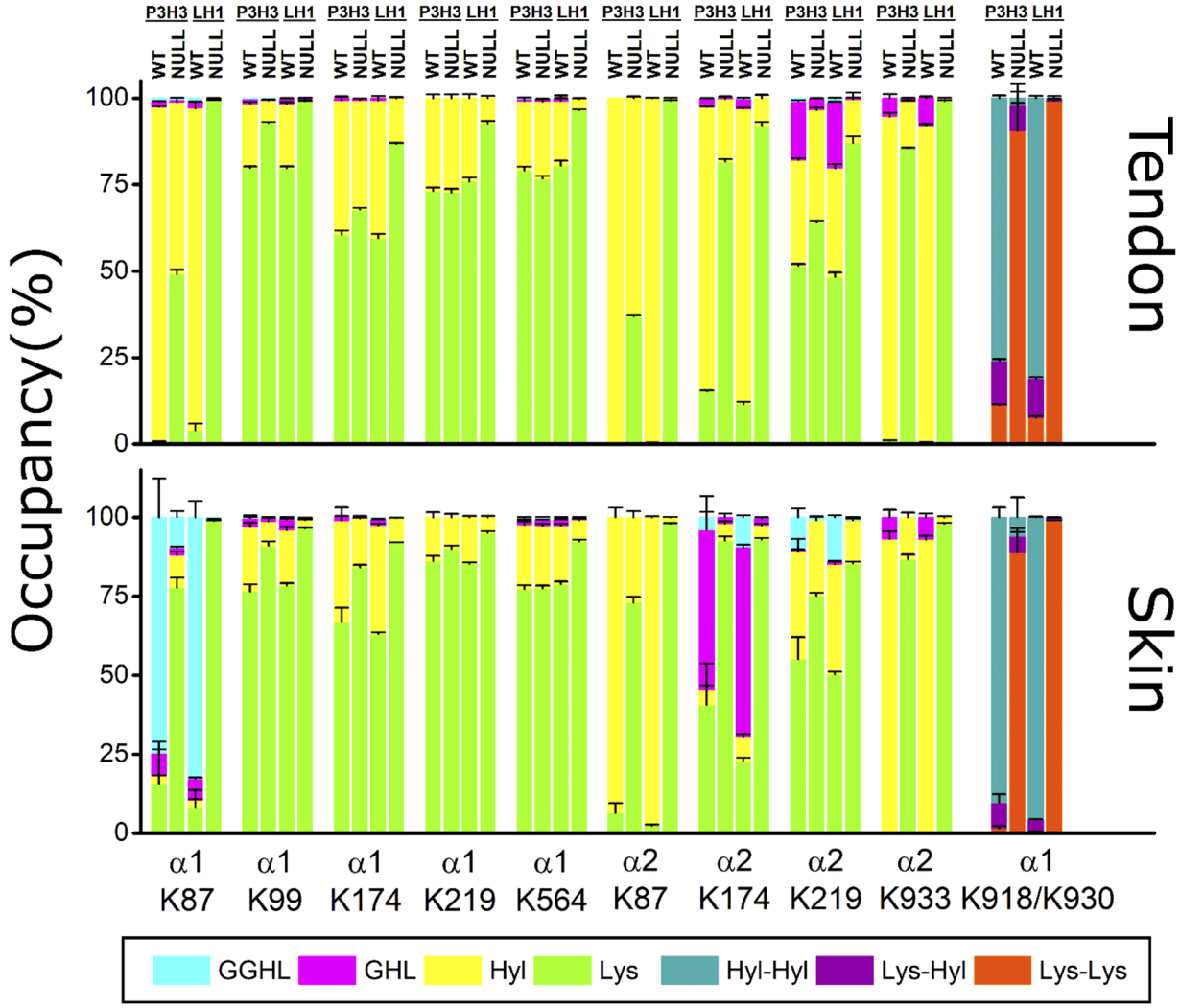

755

756

757 **Figure 6**

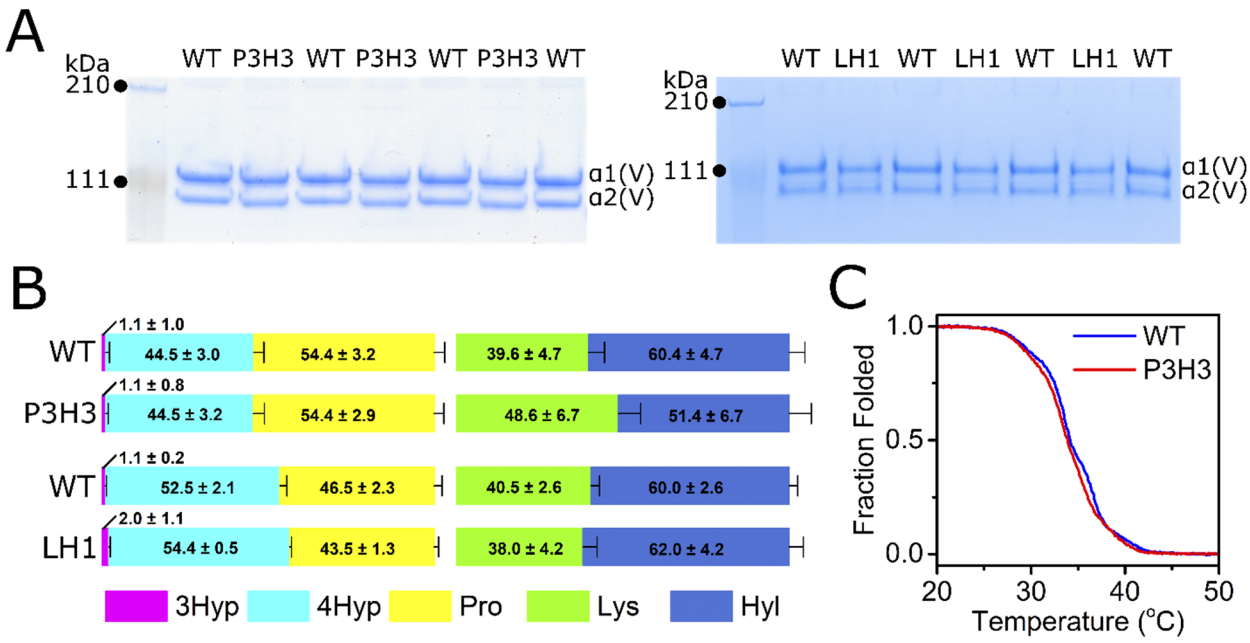

758

759

760 **Figure 7**

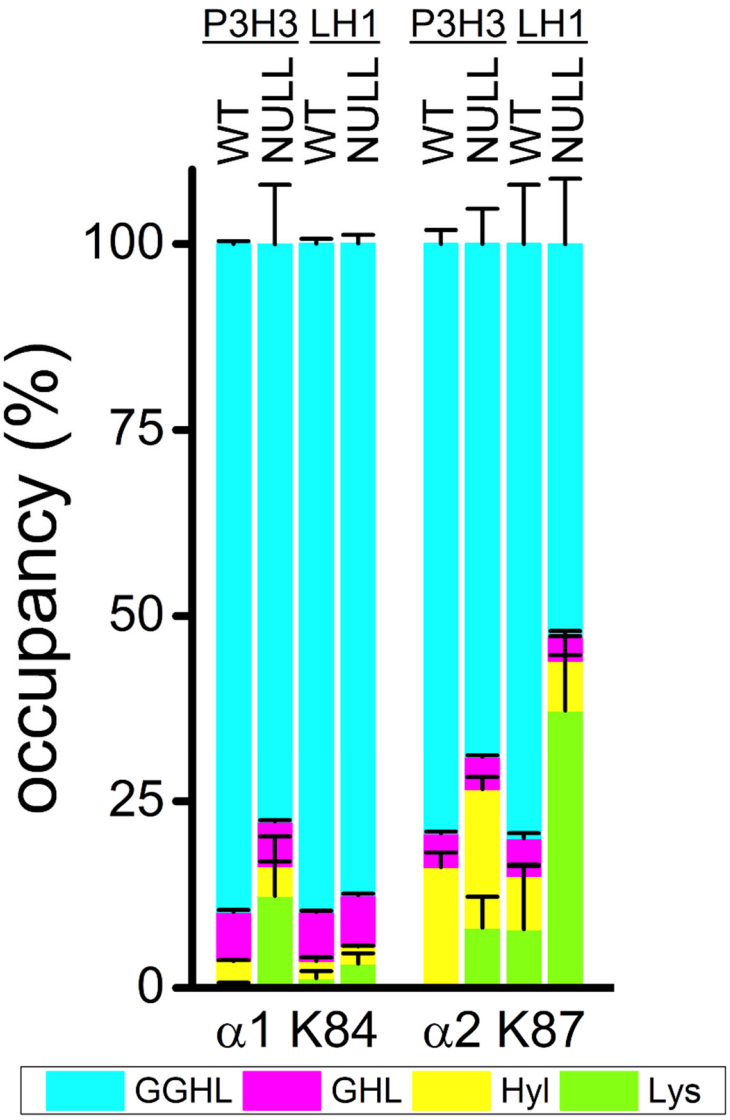

761

762

763 **Figure 8**

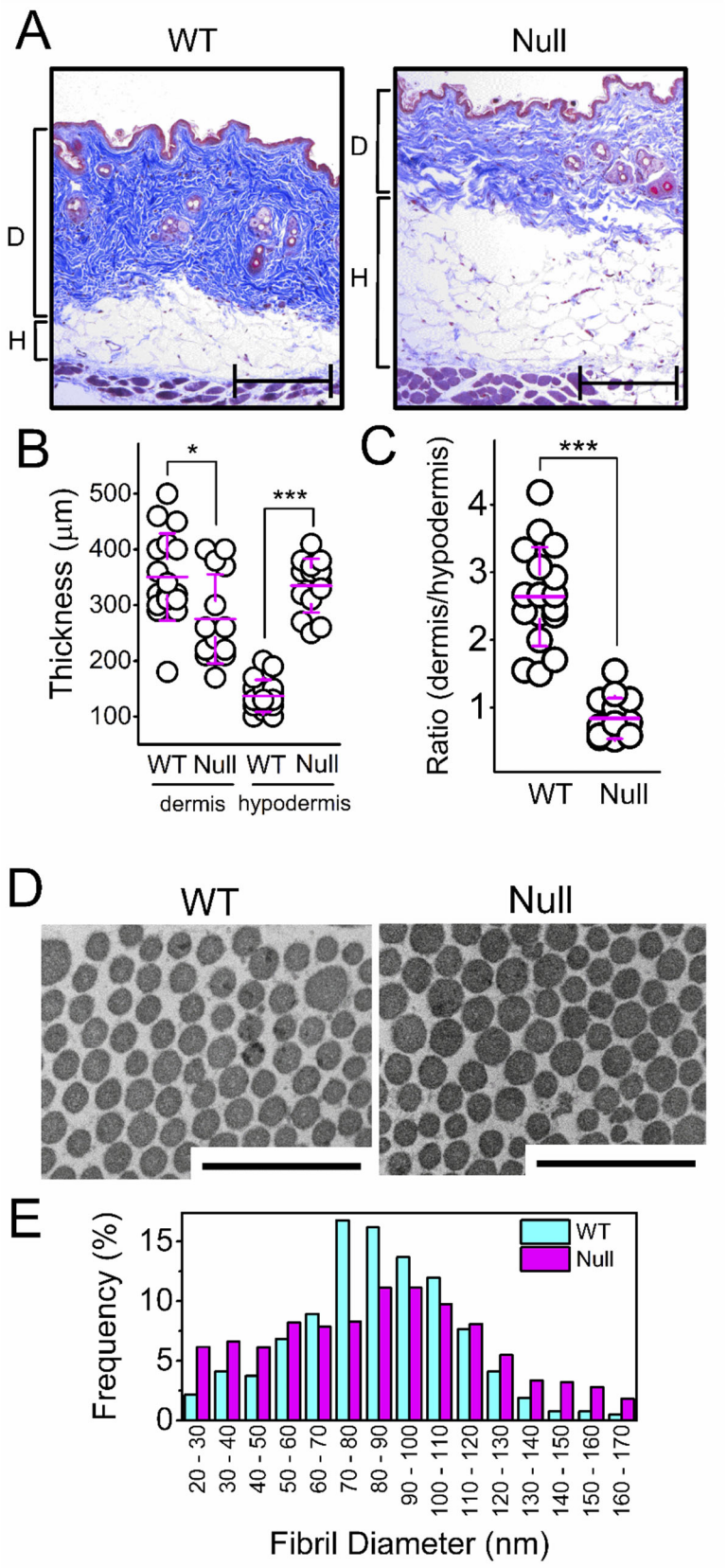

764

765 **Figure 9**

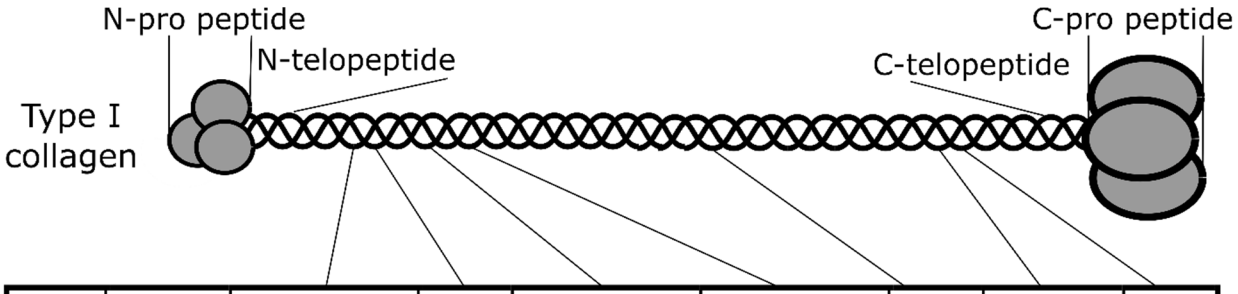

	residue	K87		K99	K174		K219		K564	K918/K930	K933
	chain	α1	α2	α1	α1	α2	α1	α2	α1	α1	α2
tendon	P3H3 null										
	LH1 null										
	CypB null			No Data					No Data	No Data	No Data
skin	P3H3 null										
	LH1 null										
	CypB null										

766

767

Figure 10

			-12			-9			-6			-3			0			3			6			9			12
col1a1	K87	human	R	G	L	P	G	T	A	G	L	P	G	M	K	G	H	R	G	F	S	G	L	D	G	A	K
		mouse	R	G	L	P	G	T	A	G	L	P	G	M	K	G	H	R	G	F	S	G	L	D	G	A	K
		bovine	R	G	L	P	G	T	A	G	L	P	G	M	K	G	H	R	G	F	S	G	L	D	G	A	K
	K99	human	K	G	H	R	G	F	S	G	L	D	G	A	K	G	D	A	G	P	A	G	P	K	G	E	P
		mouse	K	G	H	R	G	F	S	G	L	D	G	A	K	G	D	A	G	P	A	G	P	K	G	E	P
		bovine	K	G	H	R	G	F	S	G	L	D	G	A	K	G	D	A	G	P	A	G	P	K	G	E	P
	K174	human	A	G	P	P	G	F	P	G	A	V	G	A	K	G	E	A	G	P	Q	G	P	R	G	S	E
		mouse	T	G	P	P	G	F	P	G	A	V	G	A	K	G	E	A	G	P	Q	G	A	R	G	S	E
		bovine	A	G	P	P	G	F	P	G	A	V	G	A	K	G	E	G	G	P	Q	G	P	R	G	S	E
	K219	human	A	G	N	P	G	A	D	G	Q	P	G	A	K	G	A	N	G	A	P	G	I	A	G	A	P
		mouse	A	G	N	P	G	A	D	G	Q	P	G	A	K	G	A	N	G	A	P	G	I	A	G	A	P
		bovine	A	G	N	P	G	A	D	G	Q	P	G	A	K	G	A	N	G	A	P	G	I	A	G	A	P
	K564	human	P	G	E	P	G	A	A	G	L	P	G	P	K	G	D	R	G	D	A	G	P	K	G	A	D
		mouse	P	G	E	P	G	A	A	G	L	P	G	P	K	G	D	R	G	D	A	G	P	K	G	A	D
		bovine	P	G	E	P	G	A	A	G	L	P	G	P	K	G	D	R	G	D	A	G	P	K	G	A	D
	K918	human	R	G	P	A	G	P	Q	G	P	R	G	D	K	G	E	T	G	E	Q	G	D	R	G	I	K
		mouse	R	G	P	A	G	P	Q	G	P	R	G	D	K	G	E	T	G	E	Q	G	D	R	G	I	K
		bovine	R	G	P	A	G	P	Q	G	P	R	G	D	K	G	E	T	G	E	Q	G	D	R	G	I	K
	K930	human	K	G	E	T	G	E	Q	G	D	R	G	I	K	G	H	R	G	F	S	G	L	Q	G	P	P
		mouse	K	G	E	T	G	E	Q	G	D	R	G	I	K	G	H	R	G	F	S	G	L	Q	G	P	P
		bovine	K	G	E	T	G	E	Q	G	D	R	G	I	K	G	H	R	G	F	S	G	L	Q	G	P	P
col1a2	K87	human	R	G	F	P	G	T	P	G	L	P	G	F	K	G	I	R	G	H	N	G	L	D	G	L	K
		mouse	R	G	F	P	G	T	P	G	L	P	G	F	K	G	V	K	G	H	S	G	M	D	G	L	K
		bovine	R	G	F	P	G	T	P	G	L	P	G	F	K	G	I	R	G	H	N	G	L	D	G	L	K
	K174	human	A	G	P	P	G	F	P	G	A	P	G	P	K	G	E	I	G	A	V	G	N	A	G	P	A
		mouse	A	G	P	P	G	F	P	G	A	P	G	P	K	G	E	L	G	P	V	G	N	P	G	P	A
		bovine	A	G	P	P	G	F	P	G	A	P	G	P	K	G	E	L	G	P	V	G	N	P	G	P	A
	K219	human	P	G	N	P	G	A	N	G	L	T	G	A	K	G	A	A	G	L	P	G	V	A	G	A	P
		mouse	P	G	N	P	G	T	N	G	L	T	G	A	K	G	A	T	G	L	P	G	V	A	G	A	P
		bovine	P	G	N	P	G	A	N	G	L	P	G	A	K	G	A	A	G	L	P	G	V	A	G	A	P
	K933	human	P	G	E	K	G	P	R	G	L	P	G	L	K	G	H	N	G	L	Q	G	L	P	G	I	A
		mouse	P	G	D	K	G	H	R	G	L	P	G	L	K	G	Y	S	G	L	Q	G	L	P	G	L	A
		bovine	P	G	D	K	G	P	R	G	L	P	G	L	K	G	H	N	G	L	Q	G	L	P	G	L	A
col5a1	K84	human	R	G	F	D	G	L	A	G	L	P	G	E	K	G	H	R	G	D	P	G	P	S	G	P	P
		mouse	R	G	F	D	G	L	A	G	L	P	G	E	K	G	H	R	G	D	P	G	P	S	G	P	P
		bovine	R	G	F	D	G	L	A	G	L	P	G	E	K	G	H	R	G	D	P	G	P	S	G	P	P
col5a2	K87	human	R	G	F	P	G	A	P	G	L	P	G	L	K	G	H	R	G	H	K	G	L	E	G	P	K
		mouse	R	G	F	P	G	A	P	G	L	P	G	L	K	G	H	R	G	H	K	G	L	E	G	P	K
		bovine	R	G	F	P	G	A	P	G	L	P	G	L	K	G	H	R	G	H	K	G	L	E	G	P	K